Thesis

The clinical value of a dual-staged [^{18}F]FDG PET/CT protocol in diagnosing cardiac sarcoidosis in a retrospective study

submitted by

Pero Ravnjak

in partial fulfillment of the requirements for the degree of

Doktor der gesamten Heilkunde

(Dr. med. univ.)

at the

Medical University of Graz

executed at the

Department of Radiology

Division of Nuclear Medicine

under the supervision of

OÄ^{in}. Dr^{in}. Birgit Pernthaler

Univ.-Ass. Dr. Friedrich Weitzer

Univ.-Prof.^{in} Dr.^{in} Reingard Maria Aigner

Graz, July 5th, 2024

Declaration of Academic Integrity

I hereby confirm that the present diploma thesis is the result of my own independent scholarly work. I also confirm that in all cases, where material from the work of others (in books, articles, essays, dissertations, and on the internet) is acknowledged, quotations and paraphrases are clearly indicated. No material other than that cited in the reference list has been used. I have read and understood the Medical University of Graz's regulations and procedures concerning plagiarism.

Graz, July 5th, 2024 Pero Ravnjak m.p.

Danksagungen

Mein Engel, der mich durch all diese Zeit geleitet hat, mein seliger Ante. Ich danke dir für all die Kraft, die du mir auf irdischer Basis schenktest und nach deinem plötzlichen Ableben, in geistiger Form gibst. All den Ballast der Welt und meine alltäglichen Sorgen hast du mir abgenommen, ich vermisse dich sehr, jedoch warst du nie weg, denn in meinen Gedanken und Erinnerungen lebst du für immer weiter. Du bist und bleibst immer in meinem Herzen, jetzt und auf ewig, ich liebe dich.

Viel Liebe und Dankbarkeit geht an meine Familie, die mich tatkräftig beim Studium und Erstellen der Diplomarbeit unterstützte. Meine Eltern, Nada und Branko, die mir trotz Flucht aus der kriegszerstörten Heimat, ein gutes Leben schaffen konnten. Meine Geschwister, Ružica, Isidora, Stijepo und Ante, danke euch für euer leidenschaftliches Mitfiebern, Mitzittern und Mitfreuen, unabhängig davon was gerade anstand. Ich liebe euch.

Ein großes Dankeschön gebührt meiner besten Freundin Nikol, die sich trotz des fachfremden Inhaltes immer die Zeit nahm, um sich meine Arbeit zu lesen und mich aufzumuntern weiterzumachen und nicht aufzugeben, unabhängig der Hürden. Thank you, my bestie, love you.

Ein großes Dankeschön geht auch an die Betreuung meiner Diplomarbeit, OÄ^{in}. Dr^{in}. Birgit Pernthaler, Univ.-Ass. Dr. Friedrich Weitzer und Univ.-Prof.^{in} Dr.^{in} Reingard Maria Aigner. Ich danke Ihnen, dass Sie mich nicht aufgegeben haben und Sie sich die Zeit genommen haben, mir jeden Schritt der medizinischen Forschung näher zu erläutern. Ich wünsche Ihnen viel Erfolg in der weiteren Berufslaufbahn und im anstehenden Ruhestand.

Zu guter Letzt, danke an meinen Freund Dominik. Du warst, unabhängig der Umstände, immer für mich da. In den Stürmen des Lebens warst und bist du mein Fels in der Brandung. In dieser Odyssee des Lebens hast du mich geleitet und zu einem besseren Menschen gemacht, ich liebe dich.

Zusammenfassung

Titel: Wertigkeit eines zweizeitigen [^{18}F]FDG PET/CT Aufnahmeprotokolls in der Diagnostik der kardialen Sarkoidose in einer retrospektiven Analyse.

Hintergrund: Die kardiale Sarkoidose (CS) ist eine lebensbedrohliche Erkrankung, oft unterdiagnostiziert mit höherer Inzidenz als antizipiert. Etablierte Richtlinien beziehen verschiedenste Untersuchungsmodalitäten mit ein, unter anderem die Myokardbiopsie, die oft inkonklusive Ergebnisse liefert. Das [^{18}F]FDG PET/CT als nicht invasive nuklearmedizinische Untersuchungsmodalität etablierte sich zuletzt als wertvolles diagnostisches Mittel in der Detektion der CS. Hierzu ist jedoch eine spezifische Patient*innenvorbereitung erforderlich, um die physiologische Tracer-Aufnahme im Myokard zu unterdrücken. In der Literatur werden diverse [^{18}F]FDG PET/CT Untersuchungsprotokolle angeführt, weswegen in dieser Studie das an unserer Abteilung etablierte zweizeitige Akquisitionsprotokoll evaluiert wurde.

Patient*innen und Methoden: Retrospektive Datenanalyse von 219 Patient*innen mit Verdacht auf Sarkoidose. Die Vorbereitung der Patient*innen bestand aus einer mindestens 48 Stunden andauernden kohlenhydratarmen Diät mit zusätzlichem, zwölfstündigen Fasten vor der Untersuchung. Fünfzehn Minuten vor [^{18}F]FDG-Applikation wurde Heparin i.v. bei allen Patient*innen mit nichtvorhandener Antikoagulation appliziert. Das zweizeitige [^{18}F]FDG PET/CT Protokoll mit einer frühen Aufnahme des Thorax mit Fokus auf das Herz 45 min p.i. (47.33 ± 4.57 Minuten) und einer späten Aufnahme des Ganzkörpers 90 min p.i. (92.00 ± 4.36 Minuten) wurde bei allen Patient*innen durchgeführt.

Ergebnisse: Von den ursprünglich 219 Patient*innen mit der Zuweisungsdiagnose „Sarkoidose“ wurden 65/219 mit Hinweis auf CS eingeschlossen. 143/219 wurden wegen fehlenden Hinweisen auf CS und 8/219 wegen inadäquaten Untersuchungsvorbereitung ausgeschlossen. Von den eingeschlossen Patient*innen zeigten 15/65 (23.1%) einen pathologischen Tracer-Uptake im Myokard und wurden im [^{18}F]FDG PET/CT als positiv auf CS gewertet, während 50/65 (76.9%) Patient*innen aufgrund des fehlenden [^{18}F]FDG-Tracer-Uptakes im Myokard als negativ auf CS gewertet wurden. Von den fünfzehn [^{18}F]FDG-PET positiven Patient*innen, konnte in 2/15 (13.3%) eine CS bioptisch verifiziert

werden, während 6/15 (40%) Patient*innen bioptisch negativ waren und 7/15 (46.7%) Patient*innen sich keiner Biopsie unterzogen haben.
Aus dem Kollektiv an fünfzig PET negativen Patient*innen, unterzogen sich 12/50 (24%) Patient*innen einer Biopsie, die in allen Fällen als negativ zu werten war. Auf Sarkoidose verdächtige Läsionen fanden sich [^{18}F]FDG PET in den meisten Fällen im linken Ventrikel 13/15 (87%), im Septum 11/15 (73%), im Apex 7/15 (47%), im rechten Ventrikel 6/15 (40%) und den Papillarmuskeln 4/15 (27%). Von den fünfzehn PET positiven Patient*innen, erhielten 12/15 (80%) Patient*innen in idealtypischer Form vorbereitend gewichtsadaptiert Heparin zur Unterdrückung des physiologischen myokardialen Uptake während bei 3/15 (20%) Patient*innen aufgrund vorbestehender Antikoagulation darauf verzichtet wurde. Bei diesen Patient*innen zeigten sich Unterschiede in der myokardialen Traceraufnahme semiquantifiziert mit SUVmax. Patient*innen mit Heparingabe zeigten in den Frühaufnahmen (6,43 ± 1,39) als auch in den Spätaufnahmen (8,04 ± 1,63) einen geringeren myokardialen SUVmax als Patient*innen ohne Heparingabe, mit den Frühaufnahmen (8,88 ± 1,21) und den Spätaufnahmen (11,91 ± 4,29).

Conclusio: Die 15/65 [^{18}F]FDG PET positiven Patient*innen zeigten im zweizeitigen Untersuchungsprotokoll myokardialen Uptake, somit auf CS suspekte Befunde. Die 50/65 [^{18}F]FDG PET negativen Patient*innen zeigten sowohl in den Frühaufnahmen als auch in den Spätaufnahmen keinen myokardialen Uptake. Bei allen 15 PET positiven Patient*innen konnte die CS bereits in den frühen Aufnahmen diagnostiziert werden. Der höhere pathologische myokardiale Tracer-Uptake in den Spätaufnahmen ermöglicht aufgrund der höheren Tissue-to-Blood-Ratio die bessere Diagnostik der CS. Die Spätaufnahmen hatten den Vorteil, dass weitere Sarkoidoseherde im gesamten Körper dargestellt wurden, im Gegensatz zum begrenzten Aufnahmefeld der Frühaufnahmen, das sich nur auf den Thorax konzentrierte. Zusätzlich zeigten Patient*innen mit Heparingabe eine bessere Unterdrückung der physiologischen [^{18}F]FDG-Resorption (mit einem TBR von 3.29 ± 0.65) im Vergleich zu Patient*innen ohne Heparingabe (mit einem TBR von 4.80 ± 1.26). Aufgrund der in dieser Studie gewonnenen Ergebnisse ist der Mehrwert des zweizeitigen Untersuchungsprotokolls nicht gegeben. Somit ist der Verzicht auf die Frühaufnahmen gerechtfertigt.

Abstract

Title: The clinical value of a dual-staged [^{18}F]FDG PET/CT protocol in diagnosing cardiac sarcoidosis in a retrospective study.

Background: CS is a life-threatening illness, mostly underdiagnosed and affecting more people with sarcoidosis than initially believed. Established recommendations, with a variety of diagnostic approaches for diagnosing CS exist, including the myocardial biopsy, which often provides inadequate results. The [^{18}F]FDG PET/CT, as a non-invasive nuclear medicine examination modality, has recently established itself as a valuable diagnostic tool in the detection of CS. However, this modality requires specific patient preparation to suppress the physiological tracer uptake in the myocardium. Various [^{18}F]FDG PET/CT examination protocols exist, therefore we evaluated the dual-staged acquisition protocol from our department.

Patients and Methods: Retrospective analysis of 219 patients with suspected sarcoidosis. The preparation of the patients consisted of a low-carbohydrate diet lasting at least 48 hours with an additional twelve-hour fast prior to the examination. Heparin i.v. was administered to all of the patients, with no other form of anticoagulation, fifteen minutes before [^{18}F]FDG application. The dual-staged [^{18}F]FDG PET/CT protocol with an early image of the thorax focusing on the heart 45 min p.i. (47.33 ± 4.57 minutes) and a late whole-body image 90 min p.i. (92.00 ± 4.36 minutes) was carried out on all patients.

Results: Out of the original 219 patients with the assigned diagnosis “sarcoidosis”, 65/219 were included due to the suspicion of CS. 143/219 were excluded due to a lack of clinical and diagnostic evidence of CS and an additional 8/219, due to inadequate examination preparation. From the included patients, 15/65 (23.1%) showed pathological tracer uptake in the myocardium in the [^{18}F]FDG PET/CT, while 50/65 (76.9%) patients were considered negative due to the absence of pathological tracer uptake in the myocardium in their respective scans. Out of the fifteen PET positive patients with CS, only 2/15 (13.3%) had a biopsy verified CS, while 6/15 (40%) patients were considered negative by the biopsy, and 7/15 (46.7%) patients did not undergo biopsy. From the collective of fifty PET-negative

patients, 12/50 (24%) patients underwent a biopsy, which was assessed as negative in all cases.

Lesions suspicious for sarcoidosis in the [^{18}F]FDG PET in our patient population showed that in most cases the left ventricle 13/15 (87%), the septum 11/15 (73%), the apex 7/15 (47%), the right ventricle 6/15 (40%) and the papillary muscles 4/15 (27%) were affected. From the fifteen PET-positive patients, 12/15 (80%) patients received weight-adapted heparin to suppress the physiological myocardial uptake and 3/15 (20%) patients abstained of receiving heparin due to their existing anticoagulation. Differences were found in these patients in myocardial tracer uptake semi-quantified with SUVmax. Patients given heparin showed a lower myocardial SUVmax uptake in both early images (6.43 ± 1.39) and late images (8.04 ± 1.63) than patients who received other anticoagulants, with their respective early (8.88 ± 1.21) and late images (11.91 ± 4.29).

Conclusion: The 15/65 [^{18}F]FDG PET positive patients showed myocardial uptake in their dual-staged protocol, fitting for CS suspicious findings. The 50/65 [^{18}F]FDG PET negative patients showed no myocardial uptake in both the early and late imaging. In all 15 PET-positive patients, CS was able to be diagnosed already in the early images. The higher pathological myocardial tracer uptake in the late images facilitated diagnosis of CS possible due to the higher tissue-to-blood ratio. The late images had the advantage of showing additional foci of sarcoidosis throughout the whole body, in contrast to the smaller image field of the early images, which only focused on the thorax. In addition, patients with heparin administration showed better suppression of physiological [^{18}F]FDG uptake (with a TBR of 3.29 ± 0.65) compared to patients without heparin administration (with a TBR of 4.80 ± 1.26). Based on the results obtained in this study, the additional value of the early images in the dual-staged examination protocol is not given. Therefore, abandoning the early scanning procedure is justified.

Declaration of previous publications

I hereby declare that I have not published any form of scientific work prior to writing this thesis.

Table of contents

Abbreviations and their explanations

NCG	non-caseating granulomas
CS	cardiac sarcoidosis
ICS	isolated cardiac sarcoidosis
VA	ventricular arrhythmias
HF	heart failure
TNFA2	tumor necrosis factor allele 2
SAA	serum amyloid A
EMB	endomyocardial biopsy
ECS	extra-cardiac sarcoidosis
AVB	atrioventricular block
SCD	sudden cardiac death
LVEF	left ventricular ejection fraction
ECG	Electrocardiogram
CMR	cardiac magnetic resonance imaging
PET/CT	positron emission tomography/computed tomography
BBB	bundle branch block
TTE	transthoracic echocardiography
LGE	late gadolinium enhancement
ACE	angiotensin-converting enzyme
sIL-2R	soluble interleukin-2 receptor
BNP	B-type natriuretic peptide
[^{18}F]FDG PET/CT	[^{18}F]FDG positron emission tomography/computed tomography
[^{18}F]FDG	2-[^{18}F]fluoro-2-deoxyglucose
keV	kilo-electron volts
LOR	line of reception
SUV	standardized uptake value
FFA	free fatty acids
GLUT	glucose transporter
I.U.	International units
i.v.	Intravenous
p.i.	Post injection

DGP	Deutsche Gesellschaft für Pneumonologie und Beatmungsmedizin
DGK	Deutsche Gesellschaft für Kardiologie – Herz- und Kreislaufforschung
JMHW	Japanese Ministry of Health and Welfare
JCS	Japanese Circulation Society
HRS	heart rhythm society
AFOV	axial field of view
PACS	picture archiving and communication system
MBq	megabecquerel
SUVmax	maximal standardized uptake value
TBR	tissue to blood ratio

List of Figures

List of Tables

1. Introduction

1.1. Cardiac sarcoidosis

Sarcoidosis is a multisystem disorder with an idiopathic onset, evolution, and in rare cases (in about 1 to 8%) lethal outcome, characterized by non-caseating granulomas (NCG) (1,2). The accumulation of NCG is abundantly seen in locations with a higher prevalence in muscle mass, hence the major involvement in the myocardium. Considering the myocardium, the strongest collection of said pathological tissue lies in the left ventricle, followed by the septum and the right ventricle, the atria coming last (3).

Although the diseases' predilection sites are the lungs, the involvement of the heart, called cardiac sarcoidosis (CS), lowers the life expectancy by a large margin (4).

Initially, the cardiac involvement in sarcoidosis consisted of 2.3%, but due to improved investigating tools, the prevalence of CS increased to 30-40% in all sarcoidosis patients (3,5,6). Concerning epidemiology of cardiac involvement in sarcoidosis, differences in ethnic groups and ages vary widely, making it hard to find a common denominator (3,7). Usually, CS is accompanied with an additional organ affected by sarcoidosis, yet in recent times the isolated cardiac sarcoidosis (ICS) has gained more importance due to its severer outcome (8).

Pathologies manifest in form of cardiac dysfunction depending on illness progression, NCG distribution extent, inflammation sites, and the disease's origin (4).

These cardiac manifestations, include heart failure (HF) or sudden cardiac death (SCD), and go as far as to enhance the five-year mortality risk to 66%, making CS the deadliest cause for all sarcoidosis patients (9).

A promising theory that may solidify the unknown etiology is a gene centered predisposition combined with a variety of antigenic noxae. The genetic baseline in patients with sarcoidosis include the tumor necrosis factor allele 2 (TNFA2) and HLA DQB*0601 (4). The noxae in place, include but are not limited to microbial and tissue antigens, which are linked to the accumulation of serum amyloid A (SAA). The SAA can be seen inside NCG with an absence of an acute inflammation (10). This genetic predisposition combined with the noxae induce an immunological reaction, leading to the production and accumulation of non-caseating inflamed NCG by an aberrant T-cell activation (1,4,10).

These NCG tend to infiltrate a variety of organs, the lungs, the heart, and the liver, leading to local and histological destruction. This damage may resolve on its own, however cardiac involvement is paired with a severer outcome if left untreated (1).

Based on a number of guidelines and recommendations, the golden standard for CS still is an endomyocardial biopsy (EMB). However using the EMB for diagnosing CS poses difficulties, as the sensitivity is lower in comparison to extra-cardiac sarcoidosis (ECS) biopsies (6).

The most common manifestations in an extent pool of CS patients were analyzed, those include in accordance with a work by De Bortoli et al. (11):

- ventricular arrhythmias (VA)
- HF
- atrioventricular block (AVB)
- SCD

All of these symptoms either directly emerge from the irreversible scarring by the infiltration of NCG or indirectly as a byproduct of a lack of treatment from the upper symptoms. Only 5% of all CS patients showcase symptoms involving the heart, aggravating a formation of a standardized protocol on when and how to test for CS.

However, as outlined by Kurmann et al. (12) medical professionals should be alerted if patients present with one or more of the following manifestations without an alternate cause to it:

- Diseases of the conductive system under the age of 60
- VA
- Left ventricular ejection fraction (LVEF) under 50%

1.2. Detection of CS

Due to its broad pattern of symptoms, a variety of examination devices examining the heart are entailed for CS diagnosing. These include but are not limited to the EMB, the electrocardiogram (ECG), the echocardiography, the cardiac magnetic resonance (CMR), biomarkers and the positron emission tomography/computed tomography (PET/CT).

EMB

The EMB is an invasive tool that helps sampling biopsies from the myocardium accessed via the venous system, entering either through the internal jugular vein or the femoral vein in Seldinger technique. The procedure itself lasts for a few minutes accompanied by imaging like ultrasound or X-ray and specimens get extracted by using a bioptome for further testing (13).

Those specimens, in regard to histology, present with NCG lesions. Macroscopically, the NCG vary from the following colors: white, yellow, brown, and grey (3).

ECG

The ECG is a non-invasive tool used to showcase the heart's function and anatomy by using the electric cardiac conductive system. The distribution of excitation in the different areas of the heart creates the ECG with its distinctive P-wave, QRS-complex and the T-wave in physiological findings (14).

If there are obstacles that prevent the distribution of the impulse, the ECG picks up this information accordingly. The obstacles in question within CS are granulomas that infiltrate the ventricular myocardium (15).

In conclusion of several studies pathologies in CS showed in ECG with the prevalence of each sign:

- SCD with up to 65%
- Bundle branch block (BBB) with up to 61%
- AVB with up to 62%
- Ventricular tachycardia with up to 42%
- Supraventricular tachycardia with up to 15% (16).

Echocardiography

The echocardiography is a non-invasive tool often used as the first instance in diagnosing CS. The symmetry and thickness of both the right and left heart, as well as the septum and pericardium get analyzed. The transthoracic echocardiography (TTE) can detect certain pathologies for a positive CS diagnosis, like:

- Reduced LVEF (<50%)
- Dilatation of the left ventricle
- Motional abnormalities in either wall
- Dysfunctional valves
- Pathological effusion of the pericardium
- Muscular dysfunctions (12).

CMR

The CMR is an imagining tool using magnetic fields for diagnosing cardiac abnormalities, like thicker myocardial walls with movement abnormalities in CS. The CMR works with either late gadolinium enhancement (LGE), which is usually done in the T1-weighted mode with the usage of gadolinium as the contrasting agent or a T2-weighted mode without the usage of a contrasting agent.

- The LGE mode shows:
    - Fibrosis
    - Scarring
    - Infiltration of pathogens
- The T2-weighted imagining mode shows:
    - Inflammation
    - Edema (17).

Biomarkers

A variety of different biomarkers has been used for trying to diagnose CS. These are extracted by drawing venous blood and include:

- angiotensin-converting enzyme (ACE)
- soluble interleukin-2 receptor (sIL-2R)
- B-type natriuretic peptide (BNP)

- Cardiac troponins

These biomarkers cover different aspects of CS. ACE and sIL2-R are more prone to be elevated in patients with a non-isolated CS. BNP and cardiac troponins, increase in conditions directly targeting the heart, such as HF and fatal arrhythmia (18). However, none of the above-mentioned biomarkers can directly pinpoint CS.

PET/CT

The PET/CT is a non-invasive functional imaging method in nuclear medicine to assess the metabolic activity in the entire body. PET uses the positron emission of various radionuclides to provide diagnostic information about various physiological and pathophysiological processes in the human body. The information is displayed visually in three-plane images (coronal, axial, sagittal). Typical radionuclides, for in-vivo usage in PET, are fluorine-18 and gallium-68, while other shorter-lived isotopes like carbon-11, oxygen-15, nitrogen-13, and rubidium-82 are less commonly used at the LKH/ Univ. Klinikum Graz (hospital of the Medical University of Graz), Department of Radiology, Division of Nuclear Medicine. A radiopharmaceutical consists of a radionuclide, which is the radioactive component, that is attached to a target substance through a linking molecule and a binding molecule as seen in Figure 1 (19).

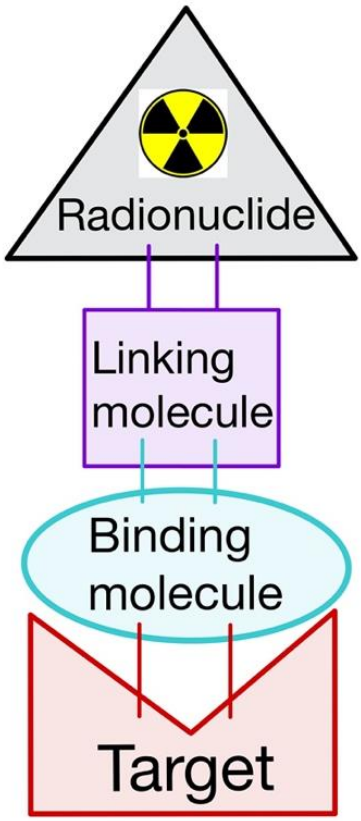

Figure 1 The composition of a radiotracer with the components needed for a functioning tracing mechanism.

The cyclotron-derived fluorine-18 allows the labelling of various molecular tracers and has a workable half-life of 109.7 min. The most common radiotracer used worldwide is fluorine-18 labelled 2-[^{18}F]fluoro-2-deoxyglucose ([^{18}F]FDG). [^{18}F]FDG accumulates like normal glucose in cells and organs with high metabolic activity therefore able to display otherwise occult neoplastic, inflammatory, and rheumatic processes. The sensitivity of the positron emission tomography/computed tomography ([^{18}F]FDG PET/CT) and its viability as a diagnostic tool in oncology and infectiology has been countlessly proven (19).

A newer and promising innovation in PET technology is the so-called digital PET using dedicated crystals to convert the annihilation rays emitted by the radiotracers directly to electrical signals without the need for photomultipliers therefore providing the ability for more counts per radioactive decays.
The radioactive decay of fluorine-18 emits a positive-charged positron, which being anti-matter is annihilated into energy when hitting a negative-charged electron.

After this impact, the inert energy of both particles is transferred into two high-energetic photons known as annihilation rays with an energy of 511 kilo-electron volts (keV) that move at light speed in two opposite directions in an 180° angle, away from the place they were created. If each photon is picked up by a detector a positive signal is counted. The time-of-flight principle is based on the difference in time of emission and admission of the radiation improving the localization of the origin and amplifying image quality.
Two factors are crucial in creating a true event, these are:

1. The origin of two gamma particles is the same annihilation event
2. The line of reception (LOR) has to be perceived as a straight line (20).

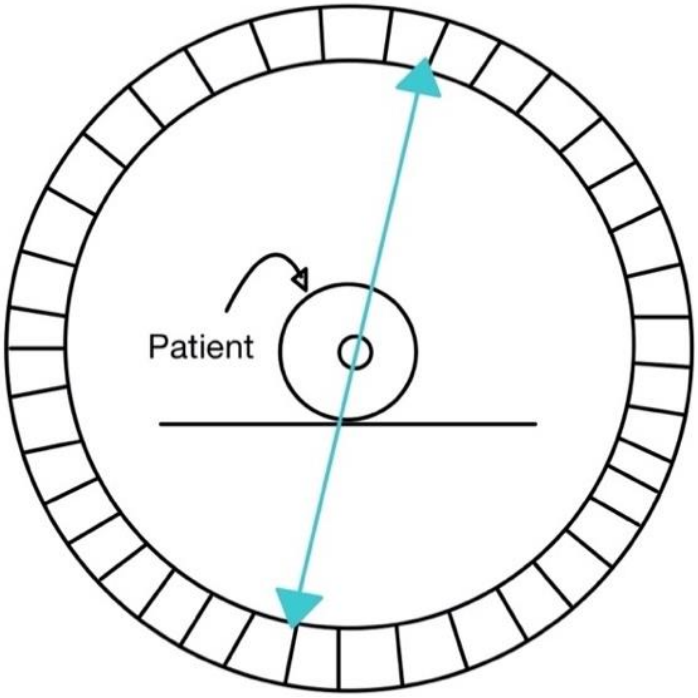

Figure 2: The line of reception (LOR) in turquoise shows a coincident event of the annihilation photons being emitted at the same position where the positron and electron annihilated. These photons then travel in 180° opposite direction.

Meaning if the photons undergo the mechanism as stated above, a coincident event takes place, which is the goal of PET scanning. Other types of events also occur that are known as false coincidence events:

- The random event. This appears in gamma rays that get detected at the same time, yet their origins of annihilation differ.

- The scattered event. Two gamma rays have the same annihilation origin. Either one or both rays get distracted on their respective ways to the detectors disrupting the creation of a straight LOR.

The CT device emits and detects X-rays from a rotating device around the patient. X-rays are weaker at around 120 keV compared to 511 keV from gamma rays (20).
For this instance scaling factors, depending on tissue density are needed to be calculated when using the CT scan for attenuation correction of the PET scan (21).
Essentially, PET and CT can be combined in one device with a single gantry, therefore the patient does not need to be repositioned to different devices during an examination. The moveable bed can be repositioned for needed imaging. Due to their different physical principles, these scans cannot be done simultaneously, thus, resulting in a short time delay. Nonetheless, thanks to the characteristics of a PET/CT-scan in contrast to the scans obtained by the devices individually, there is a considerable advantage, as the factors time and location are more precise, albeit not perfect.
CT scans also give further information of anatomical localization and pathological changes. After the scanning process, the calculated 3D images of both the PET as well as the CT can be overlapped, creating fused images. Additionally, if the weakening factors are adequately adapted and both PET and CT devices are calibrated, the data collected by the PET can lead to an absolute quantification. This means that the activity concentration for every resolved volume element (voxel) in a patient can be evaluated separately. With this data, the quantitative value can be calculated further in the form of standardized uptake value (SUV), which simply showcases the amount of distributed tracer concentration in a specific area. For an instance, if the tracer has an equal homogenous distribution, the value of SUV consists of 1, however this type of occurrence does not happen in human tissue. If this value drastically increases, higher physiological or pathological glucose accumulation and usage is assumed. Nonetheless, some organs happen to have a higher uptake based on their physiological circumstances, like the myocardium, liver, and the brain while tracer excretion via the kidneys and bladder is visible (20).
To combat this problem of physiological uptake in the myocardium, this thesis also focuses on proper patient preparations, in order to avoid errors that may falsify results.

Uptake mechanism of [^{18}F]FDG

To understand the importance of preparations used in PET/CT examining, certain physiological and pathophysiological aspects must be clarified.

In resting conditions, the heart utilizes energy derived from the oxidation of lipids, such as free fatty acids (FFA) (70% of the energy consumed), and from metabolizing glucose (30% of the energy consumed). However, pathologies, such as inflammations, increase the glucose-centered mining of energy, as the demand for said energy source is simply higher (22).

If the body finds itself in a state of reduced glucose levels, like in a diet, the heart efficiently changes its usage of energy deduced almost solely from FFA. Meaning, if the dietary restrictions are followed carefully, the human heart primarily focuses on an aerobic state of energy-mining, as the fast available energy source that is glucose, is not present. This shift in energy uptake is a major factor, as it helps to present the difference between a healthy and an inflamed heart based on their glucose demand (23).

FFA are energetic elements released by glycerides derived from two main tissue sources, which are fat and muscle. This form of energy source is being directed into the blood stream to be used by highly energy hungry organs, like the liver and in this context the heart. These FFA also undergo transformation into ketone bodies by the liver, which can also be utilized by the heart as an energetic source (24).

If, however, the levels of glucose arise in the body, then the physiological uptake of said substance is being directed by glucose transporter (GLUT) 4, whilst sick cells use GLUT1 and GLUT3. Now, if the glucose provides more energy, less FFA gets targeted for energetic consumption (24). Reason for the uptake in this pathological state is the higher need of glucose by inflamed cells, additionally to having a higher affinity to send glucose to GLUT1 and GLUT3 transporters (25).

As previously mentioned, the heart utilizes FFA for energy purposes and can mainly access energy trough this source. The myocardial FFA levels can be elevated by adding a bolus of heparin (50 international units (I.U.) per kg body weight) a few minutes prior to [^{18}F]FDG application, as heparin activates lipase, which then lead to higher FFA levels (26).

The advantage of FFA as an energy source in this case is its ability to decrease the glucose uptake in muscles ordered by insulin as well as minimizing the GLUT4 translocations to the plasma membrane (22).

Inflamed cells, as in CS, have a higher demand for energy. That means, if there is some kind of fast available energy source, such as the D-glucose mimicking [^{18}F]FDG, sick myocardium cells tend to go for that substrate (27).
The target substance is a physiological source for the body, which is usually metabolized and as a result, the radionuclide also finds itself in the tissue that metabolizes the initial target substance (19).
The radiotracer used in this setting is [^{18}F]FDG, which consists of deoxyglucose marked with the radionuclide ^{18}F.
Deoxyglucose has a hydroxyl group (-OH) at position C2 substituted with covalent bound fluorine-18, which makes it an analogue to glucose. The glycolysis, a pathway for glucose metabolizing, has the same primary steps in both sugars, however, as soon as deoxyglucose turns into deoxyfructose-6-phosphate, it cannot further metabolize in the mitochondria (28).

Due to the nature of [^{18}F]FDG, certain preparations have been introduced to help suppress the physiological uptake of [^{18}F]FDG in the myocardium in their respective PET/CT scans. These preparations contain:

- An extended fast prior to scanning
- A particular diet minimizing carbohydrate and maximizing protein and fat intake
- Applying intravenous (i.v.) heparin

The missing suppression that results from scanning without any preparations is seen in figures 3, 4, 5. This circumstance makes it vital to properly prepare prior to CS scanning in order to eliminate any physiological uptake whatsoever (29).
In cases where suppression does not take place, as seen in figures 3, 4, 5, the difficulty to properly diagnose CS rises. Thus, if the application of [^{18}F]FDG occurs in combination with previously described preparations, then in practice a sick heart can be differentiated from a healthy one by the pathological tracer uptake in PET/CT scans.

The following images show variants of physiological uptake of [^{18}F]FDG in the myocardium in CS negative patients without any dietary restrictions or heparin application prior to the scans. All of these scans were taken approximately 60 minutes p.i. of [^{18}F]FDG.
Figure 3, 4, 5 show representative scans of three patients in 3D Maximum intensity projection PET (A), axial PET (B) and axial fused PET/CT (C).

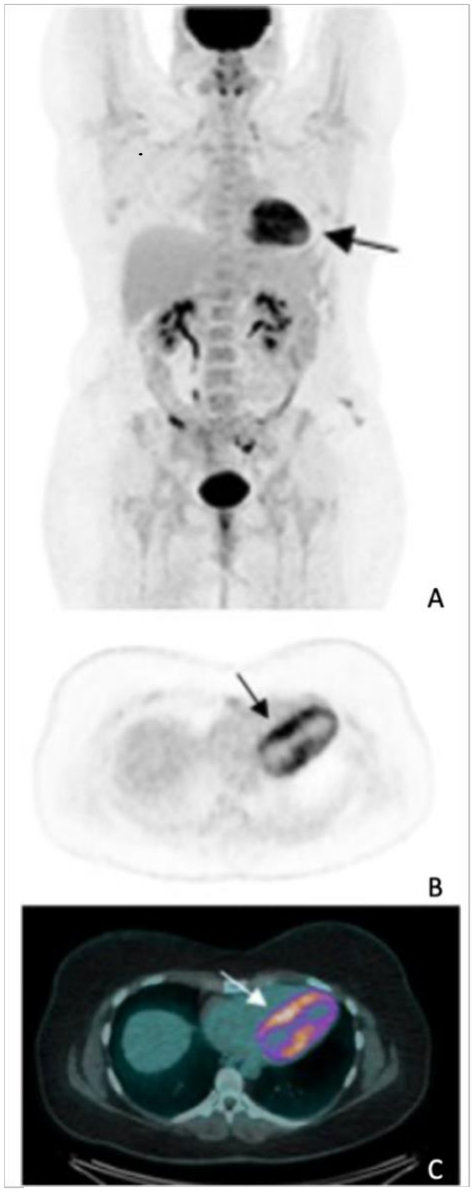

Figure 3

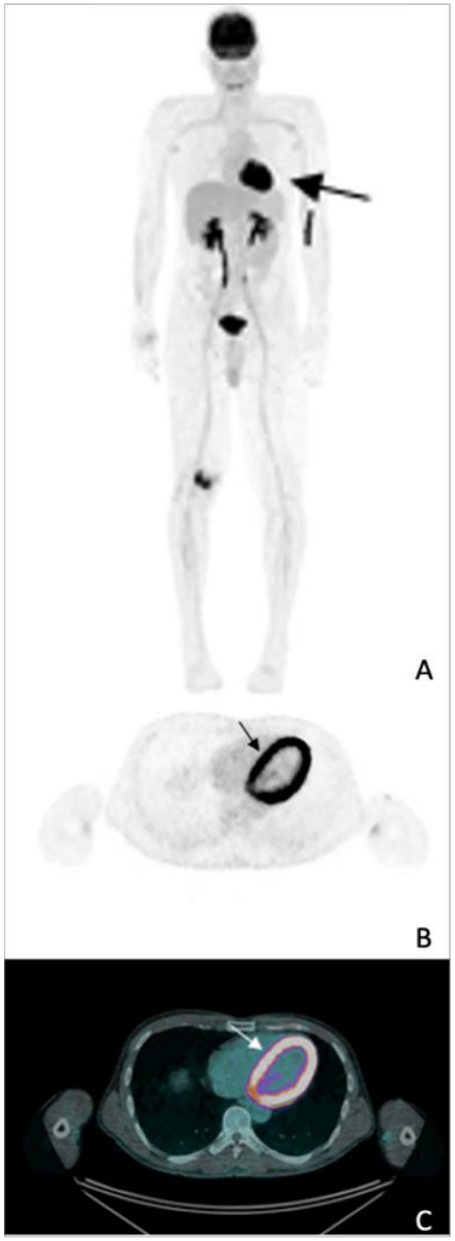

Figure 5

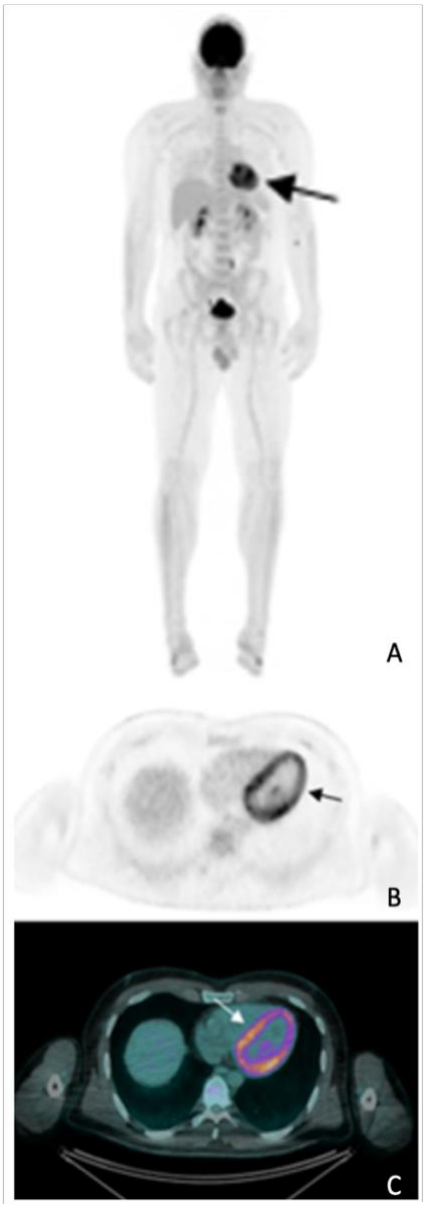

Figure 4

1.3. Established guidelines for CS diagnosing

Although the main focus in this study is the [^{18}F]FDG PET/CT, other significant examination tools for diagnosing CS are not to be ruled out. Out of all of the guidelines following, not a single one acknowledges the value of a standardized protocol for preparations and acquisition for the [^{18}F]FDG PET/CT.

In German speaking parts of Europe the recommendations for diagnosing and treating CS originate from the Deutsche Gesellschaft für Pneumonologie und Beatmungsmedizin (DGP, German Respiratory Society) and the Deutsche Gesellschaft für Kardiologie – Herz- und Kreislaufforschung (DGK, German Cardiac Society). The recommendations by DGP and DGK suggest different examination tools, depending on the presenting symptoms. There are two major groups that should be considered for further testing in those recommendations. These are:

1) people under the age of 50 with some form of cardiac pathologies without any non-CS related reasoning
2) people with preexisting ECS, that developed arrhythmias and HF later on

The first instance of tools for examining are the TTE and the ECG (either the 12 lead ECG or the 24h ECG). Pathological findings include:

- Left or right BBB
- AVB II°/III°
- Reduced LVEF (<50%)
- Pathological Q-waves in the ECG
- Ventricular tachycardia
- Abnormal thickness of the septum
- Wall motion abnormalities

If those pathologies persist, further steps include either a CMR or a PET, with a positive result leading to a high probability of CS. A follow up examination to ensure the diagnosis of a CS revolves around biopsies. These biopsies can either be of cardiac or extracardiac origin leading to the circumstance that a positive biopsy indicates cardiac involvement. This applies to the biopsy findings of every organ, even if the sarcoidosis-specific granulomas are not found in the myocardium CS is diagnosed (16).

Three different guidelines for diagnosing CS exist, which are being used outside of Europe and depending on presentation of patients.
Those are:

- Japanese Ministry of Health and Welfare (JMHW)
- Heart Rhythm Society (HRS)
- Japanese Circulation Society (JCS)

The guidelines by JCS mention [^{18}F]FDG PET/CT's ability to create better visualizations of granuloma distributions for an accurate navigation in tissue sampling. This guideline also highlights the importance of [^{18}F]FDG PET, that is why the JCS guideline will be explained in greater detail (6).
Following criteria are being used to diagnose CS according to JCS:

1. ECG abnormalities, including fatal ventricular arrhythmia and heart block
2. Irrespective of the imaging process, abnormal wall structures and thinning of the interventricular septum
3. Positive cardiac [^{18}F]FDG uptake in PET scan
4. Late gadolinium uptake in CMR
5. LVEF sinking under 50% or ventricular wall motion abnormalities

Diagnosing CS in accordance with the JCS guidelines is facilitated, if certain histological or clinical signs of ECS exist. However, a great focus is also put in the value of [^{18}F]FDG uptake in the PET scan. This nuclear medicine imaging method can diagnose an isolated CS, if ECS is not presented (30).
Both the German recommendations and the JCS mention the importance of PET/CT in diagnosing CS, however a vital aspect is not considered yet again, which is the standardized preparation protocol and the value of dual-staged scan (6,16,30).
This leads to an elevated degree of uncertainty. This circumstance leads to a variety of results in [^{18}F]FDG PET/CT scanning, which can be challenging for properly diagnosing CS.
This results in a need for a universal and standardized protocol for correctly detecting CS, which is the objective of the present thesis. The main goal was to determine the value of a two-staged [^{18}F]FDG PET/CT in diagnosing CS with a precisely defined protocol.

Furthermore, there is an inconsistency of patient protocols throughout studies that actively include [^{18}F]FDG PET/CT, which is a vital component in receiving correct and usable results, which our study also focuses on (6).

The aim of this retrospective study is to determine the clinical value of a two-time point [^{18}F]FDG PET/CT protocol in patients, who received specific preparation consisting of low carb and fat enriched diet, fasting period an i.v. unfractioned heparin application for diagnosis of suspected CS.

2. Data and Methodology

2.1. Patients and methods

This monocentric, retrospective study performed at LKH / Univ. Klinikum Graz (hospital of the Medical University of Graz), Department of Radiology, Division of Nuclear Medicine, included a total 65 patients with a suspected or radiologically verified CS. All of those patients were scanned with a [^{18}F]FDG PET/CT for solidifying the proposed diagnosis. Scans were taken from January, 1st, 2020, up until February, 1st, 2023.

Inclusion criteria in this retrospective study were:

- Myocardial uptake in the [^{18}F]FDG PET/CT scans indicating CS as analyzed by two experienced nuclear medicine physicians.
- Proper preparations including some form of blood thinner and a fat and protein-based diet lasting 48 hours
- Exceptions from heparin injection were possible for patients that take some kind of blood thinner, as injecting heparin can induce a higher chance of adverse events including bleeding
- Dual-staged [^{18}F]FDG PET/CT scans
  I. Early scans with an acquisition time 45 minutes after [^{18}F]FDG injection
  II. Late scans with an acquisition time 90 minutes after [^{18}F]FDG injection

Exclusion criteria were:

- One-staged PET/CT scans
- Suspected or verified pregnancies
- Patients with multiple scans, in this case only the first set of scans were used
- Patients without heparin or other anticoagulation
- Patients who did not stick to the diet

With these criterions in place, the patient pool of 65 participants was divided to a total of 50 PET negative patients and 15 PET positive patients. The differences of PET positive patients were also observed based on the application of intravenous heparin. 12/15 patients had an injection of heparin (50 I.U. /kg body weight) while 3/15 patients did not receive any heparin due to present oral anticoagulation, including Apixaban, Rivaroxaban, Phenprocoumon.

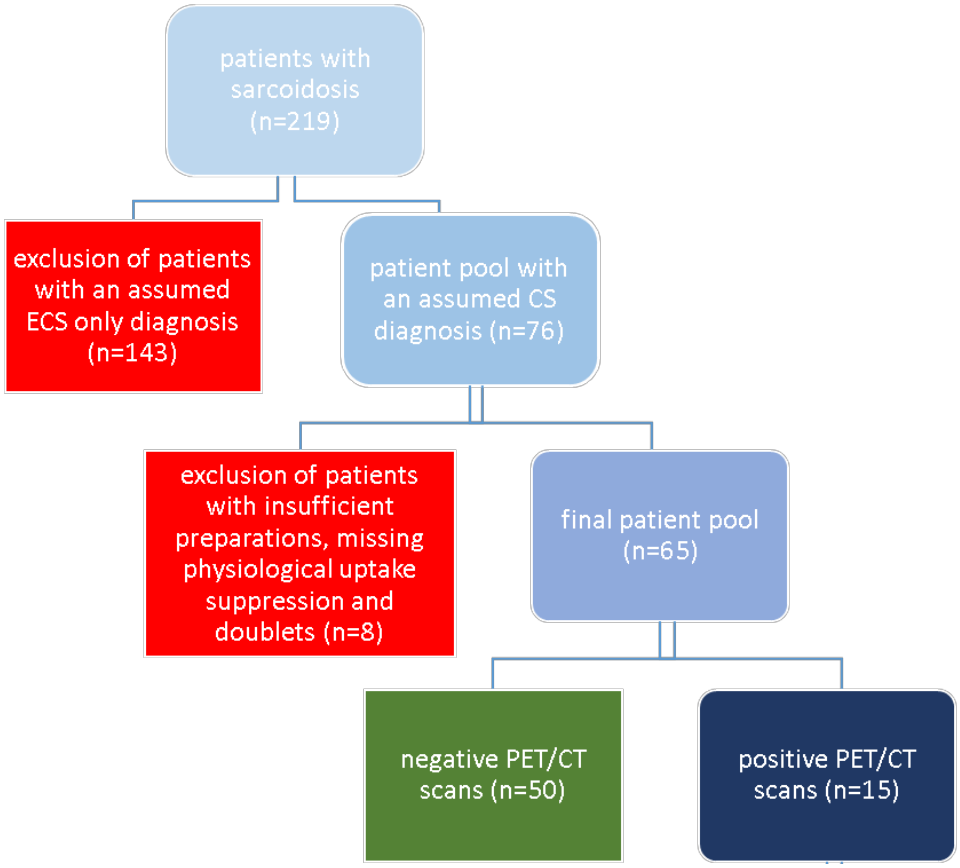

Figure 6: Flow chart for the patient selection with inclusion and exclusion criteria.

Then we compared four different parameters in [^{18}F]FDG PET/CT with their respective average as shown in Table 2.

- Myocardial SUVmax from the early images
- Myocardial SUVmax from late images
- SUVmax of the aortic arch from the late images
- Tissue to blood ratio (TBR) using the SUVmax of the mediastinal blood pool as reference

Myocardial SUVmax was measured using a volume of interest inserted (VOI) on the fused axial PET/CT images. The nuclear medicine physicians and the student reviewed the PET images and selected the [^{18}F]FDG -avid areas in the LV region. Additionally, the student recorded the results of the areas and documented these for further calculations.
To calculate the SUVmax of the blood pool needed for TBR, a VOI was drawn inside the aortic arch for background reference.

Additional data acquisition for clinical information was performed through the clinical documentation system openMEDOCS™, while study relevant information from PET scans was gathered from the in-house picture archiving and communication system (PACS).

2.2. Patient preparations

Patients were restricted to comply to a ketogenic diet for 48 hours prior to their respective scans, as patients are obliged to consume only high fat and protein-rich aliments, leaving out any kind of carbohydrate for at least 48 hours prior to scan.
Information was given in written form to prepare accordingly.

Patients are allowed to consume:

- Meat of any kind
- Eggs
- Butter, cream, and aged cheese
- Fish and sea food
- Vegetables and herbs
- Oil and fat as cooking bases
- Nuts

The following aliments should be avoided:

- Sugars of any kind, including honey, and sweets
- Carbohydrate-rich foods like bread, pastries, flour and other side dishes like rice, pasta, potatoes, couscous, bulgur
- Crisps, chips, and other salty snacks
- Legumes (beans, peas, lentils), corn and chestnuts
- Whole milk and curdled milk products like yoghurt, curd, kefir, buttermilk, and any kind of cream cheese
- Any kind of fruits and according produces like jam, fruit pulp, compote
- Sugary beverages like fruit juice, sodas, sugared tee, sugared coffee, and any kind of alcoholic beverages
- Any kind of convenience food, that may contain carbohydrates

Combined with this diet, there is a strict 12 hours fasting period prior to the scan, leaving out any kind of nourishment that is not water or unsweetened tea, meaning that the body should be deprived of any energy uptake.

Additionally, a heparin induced thrombocytopenia has to be excluded. For this, patients need to have a blood scan not older than seven days.

2.3. Imaging protocol

The early scan was performed with one bed position of the thorax focusing on the heart, while the late scan consisted of whole-body images focusing on the heart. The [^{18}F]FDG myocardial uptake in PET/CT was primary evaluated visually by two experienced nuclear medicine physicians and a medical student blinded to clinical data to avoid possible bias at the AW Workstation Server 3.2 Ext. 4.0 (GE Healthcare, Chicago, Illinois, U.S.A.). The LV myocardial [^{18}F]FDG uptake was evaluated whether the increased [^{18}F]FDG uptake was physiological or caused by active CS. In case of discordant findings, consensus was obtained. The uptake of [^{18}F]FDG was quantified by the average SUVmax in both early and late scans, as well as the tissue to blood ratio (TBR). The TBR was defined as the ratio of the myocardial SUVmax and the SUVmax of the blood pool in the aortic arch. From both the early and late scan, myocardial maximal standardized uptake value (SUVmax) was obtained via dedicated measurement tools provided by the manufacturer (AW Workstation Server Version 3.2 Ext. 4.0, GE Healthcare, Chicago, Illinois, U.S.A.).
All of the patients scanned in this study, were examined with the same PET/CT device, which is the Discovery MI Gen2 (GE Healthcare, Chicago, Illinois, U.S.A.). This device consists of a composition of 6 PET detector rings that create an Axial Field of View (AFOV) of 30 cm. Patients benefit of a lower radiation dose and a decreased scanning time, while also showcasing elevated sensitivity in detecting lesions (31).

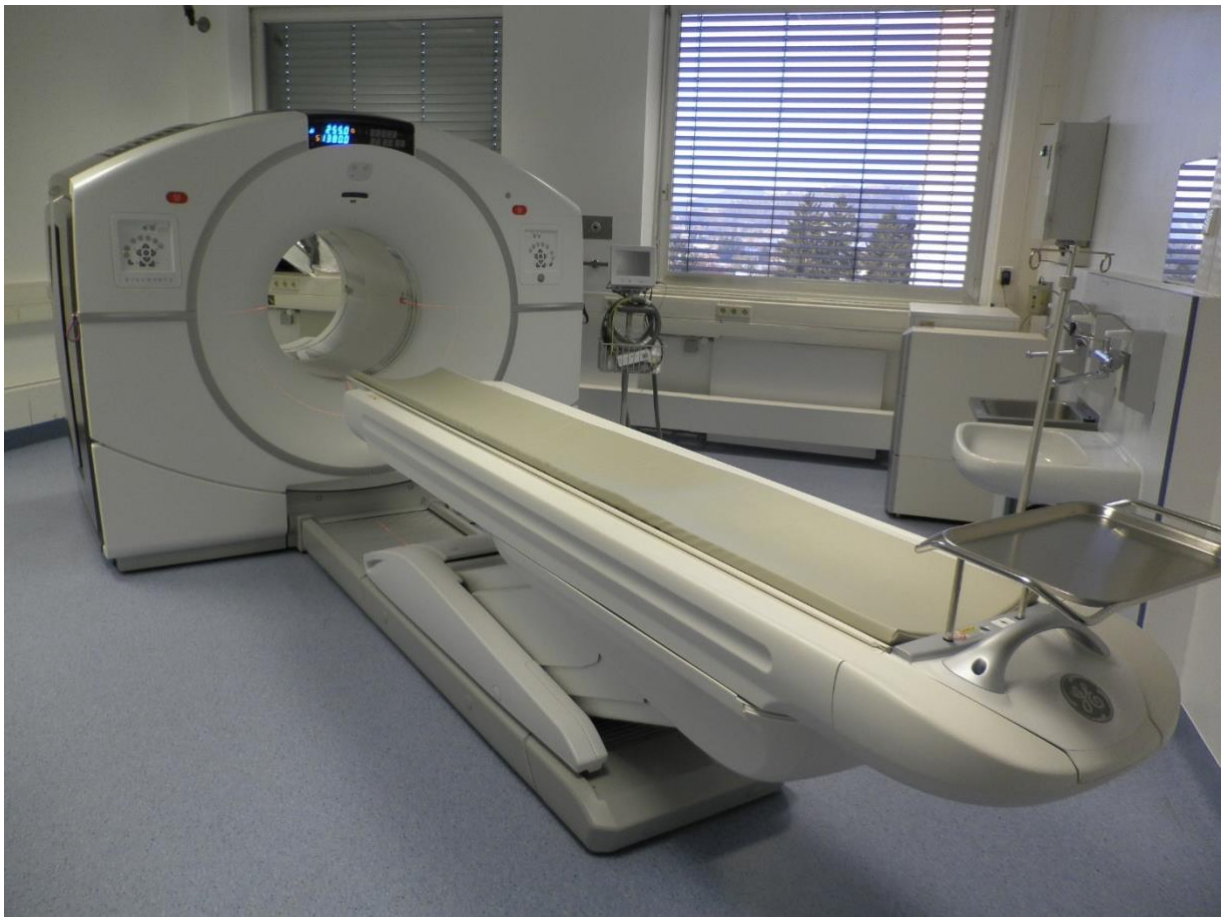

Figure 7: Discovery MI Gen 2 (GE Healthcare, Chicago, Illinois, U.S.A.) PET/CT device.

The scans are reviewed in four panels, which highlight different aspects of the PET/CT. One panel is dedicated to the CT, two are dedicated to the PET in gray-scale and one is the combination of CT and PET scans (fused images) in color using the manufacturer provided pre-set.

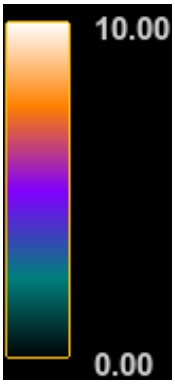

Figure 8: The legend that is in every axial fused PET/CT to display the intensity of the uptake in form of SUVmax in different colors.

After short oral anamnesis and obtaining written and oral consent, weight-dependent heparin (50 I.U. per kg bodyweight) was injected i.v. 15 minutes prior to [^{18}F]FDG application. [^{18}F]FDG was obtained by a third-party producer and injected i.v. with an activity of 2.7 megabecquerel (MBq) per kg bodyweight (maximum 284 MBq). Blood glucose levels were tested before the [^{18}F]FDG application and were required to be less than 140 mg/dl. After intravenous [^{18}F]FDG injection patients were advised to rest in a quiet, darkened, and warmed environment prior to scanning and ordered to empty their bladder before PET/CT scans were performed 45 minutes p.i. of the heart (early images) and 90 minutes p.i. of the whole body (late images) (Figure 9).

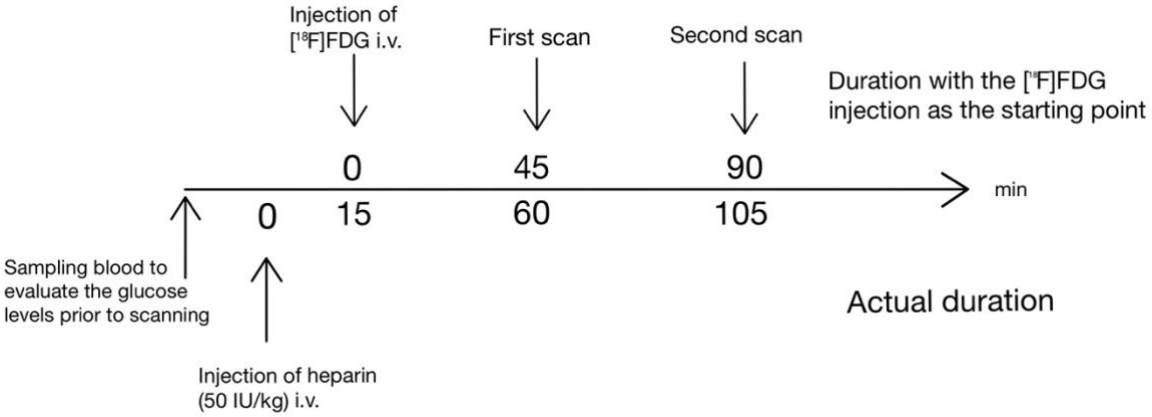

Figure 9: [^{18}F]FDG PET/CT Protocol

2.4. Assessment of information via PET scans

These following figures show important landmarks for diagnosing CS with the PET/CT. Naturally, the myocardial SUVmax is of prime interest, but the SUVmax of the blood pool in the aortic arch was also measured to adjust for background activity. This is required for the calculation of the tissue/lesion to blood pool ratio (TBR), in this case the ratio between the myocardial SUVmax and the SUVmax of the blood pool in the aortic arch.

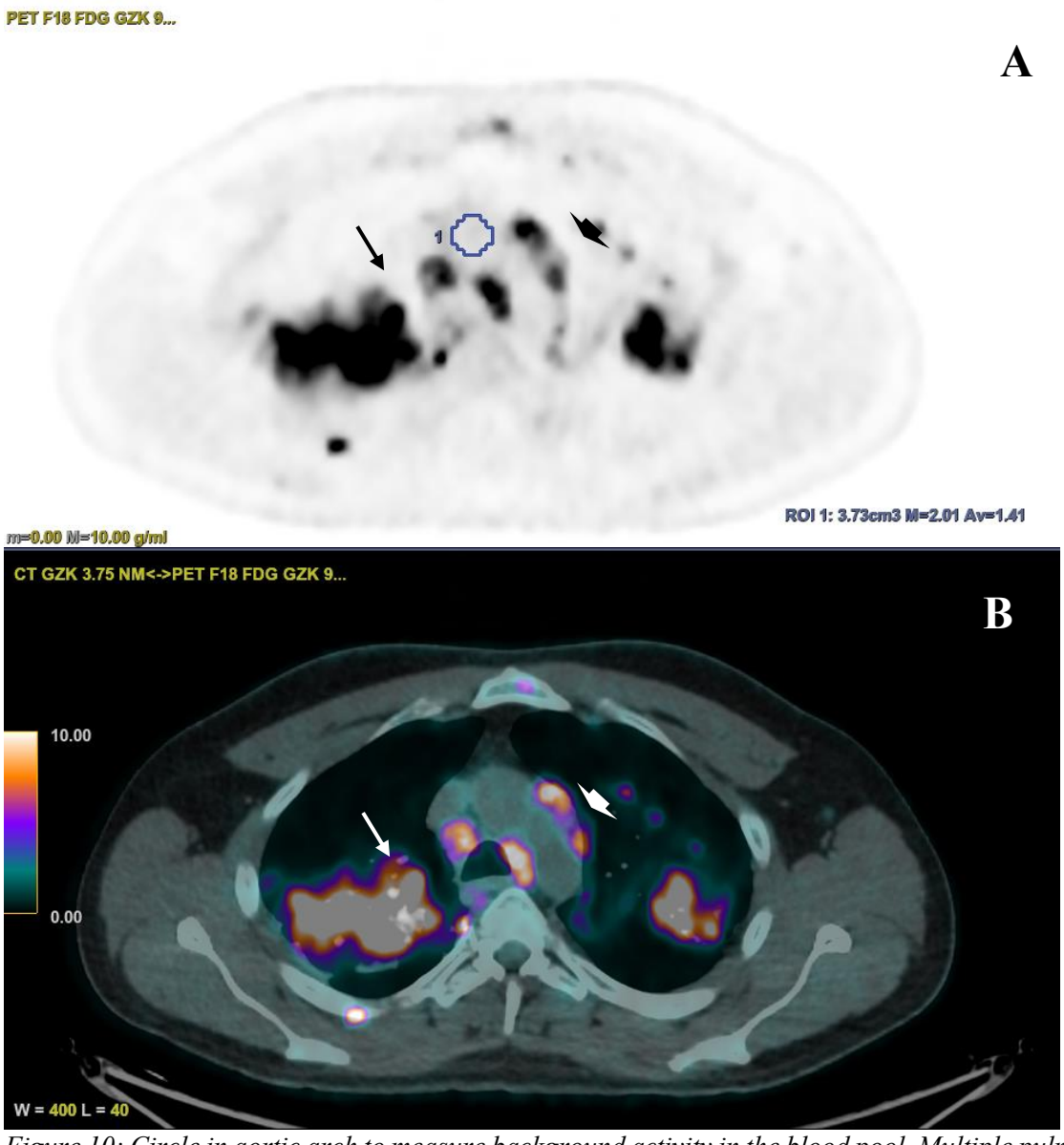

Figure 10: Circle in aortic arch to measure background activity in the blood pool. Multiple pulmonal lesions (arrow) and mediastinal lymph nodes (arrowheads) affected by sarcoidosis are present in PET mode (A) and fused images (B).

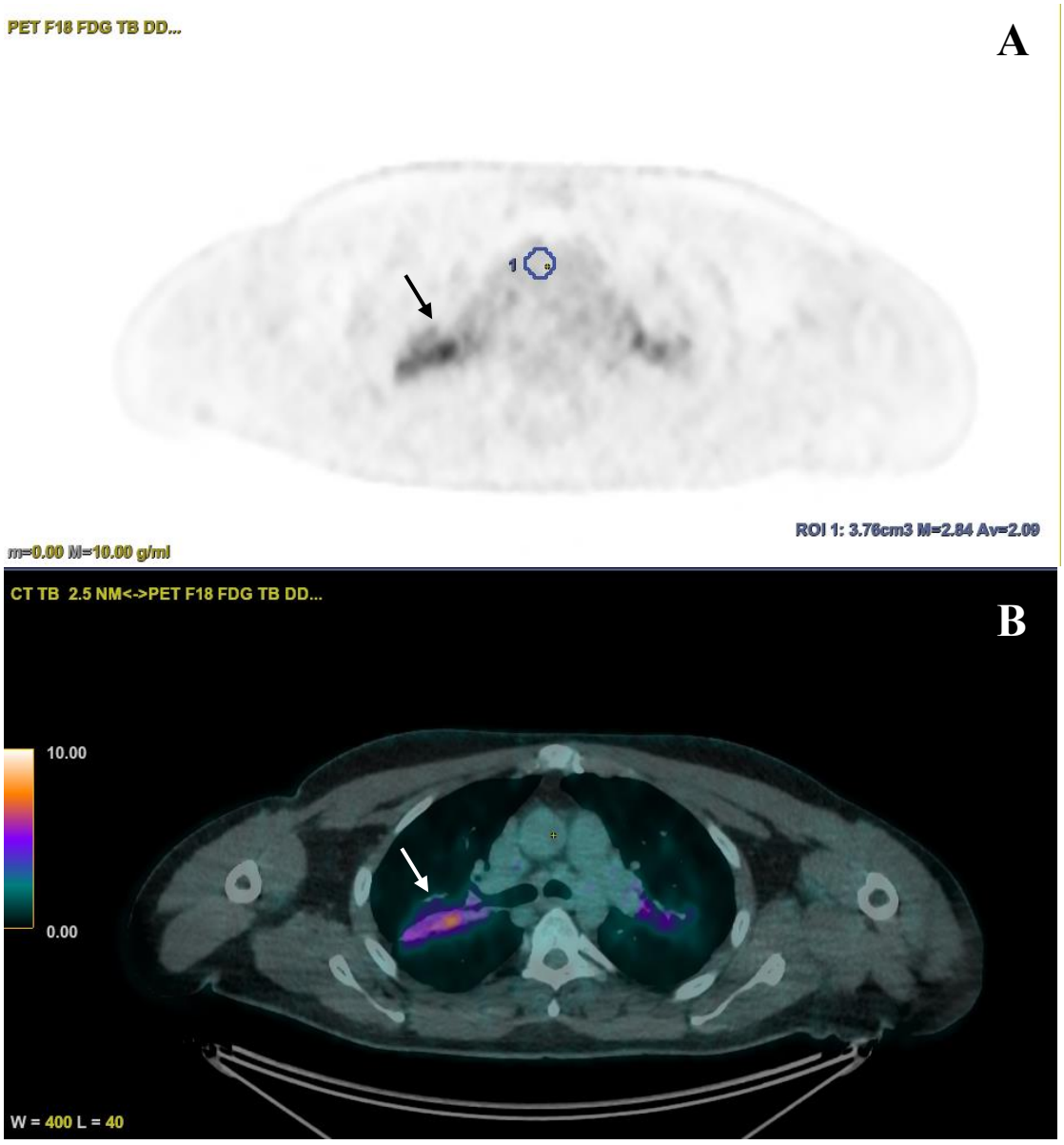

Figure 11: Follow-up examination of the patient in figure 1. Circle in aortic arch to measure background activity in the blood pool. Pulmonal lesions in partial response (arrow) and mediastinal lymph nodes in complete response in PET mode (A) and fused images (B).

A selection of scans of patients without PET/CT positive CS is displayed, however, there is a strong uptake seen in other structures. These structures mostly are the lymph nodes in the hilar area and the mediastinum. Uptake in these structures is typical for pulmonary and mediastinal sarcoidosis.

The scans are reviewed in four panels, which highlight different aspects of the PET/CT. One panel is dedicated to CT, two are dedicated to PET in gray-scale and one is the combination of CT and PET scans (fused images) in color using the manufacturer provided pre-set.

These following figures showcase the different nature of sarcoidosis in [^{18}F]FDG PET scan:

- Axial low dose CT (panel A)
- Axial fused PET/CT (panel B)
- Axial PET (panel C)
- 3D Maximum intensity projection PET (panel D)

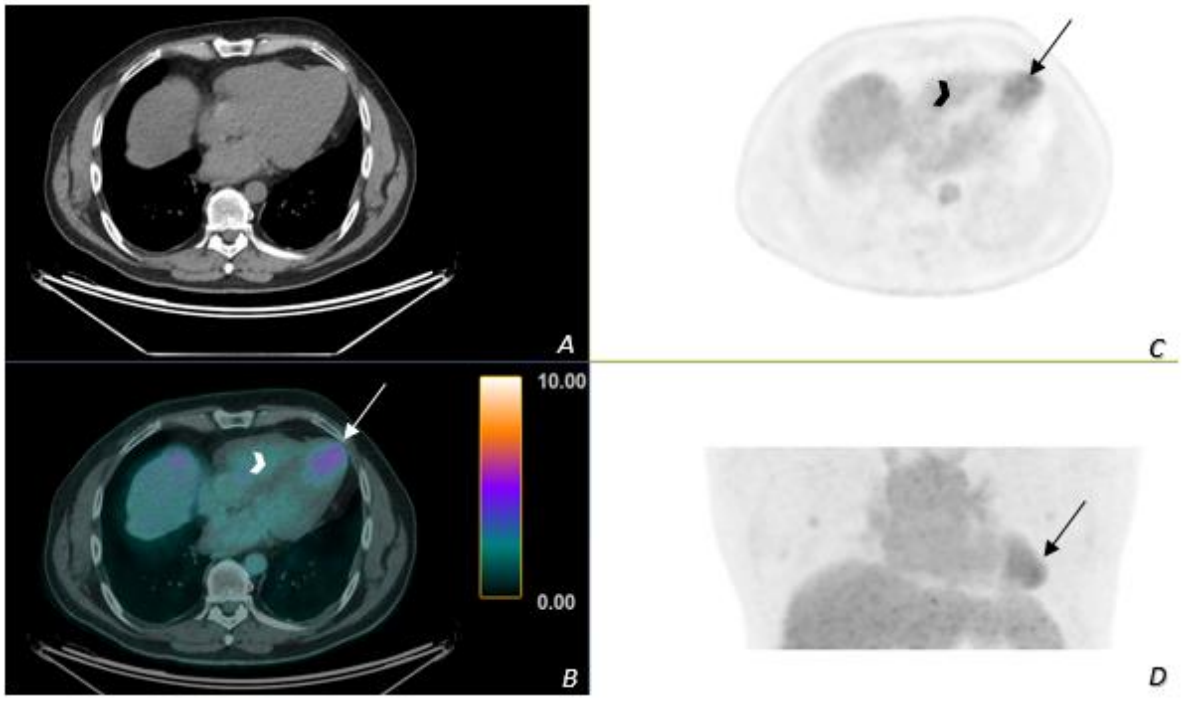

Figure 12

Figure 12: Patient with confirmed CS and prior heparin injection and dietary restrictions. In the PET scan a strong myocardial uptake in the apex (arrow) both in panel B, C and D, without any uptake in the septum (arrowhead) in panel B and C is presented.

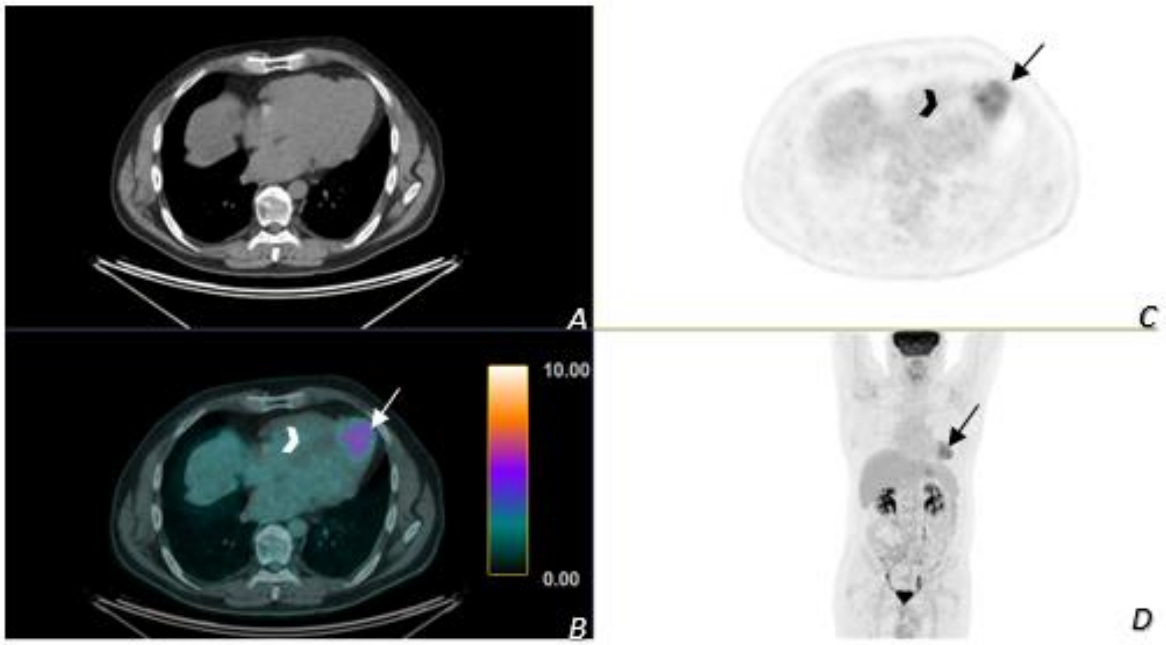

Figure 12a

Figure 12a: Same patient as in figure 12. The late acquisition shows the same myocardial uptake in the apex (arrow) in panel B, C, and D, without any uptake in the septum (arrowhead) in panel B and C. Comparing these scans with early scans in figure 12, a more intense myocardial uptake is portrayed. Less background activity is displayed.

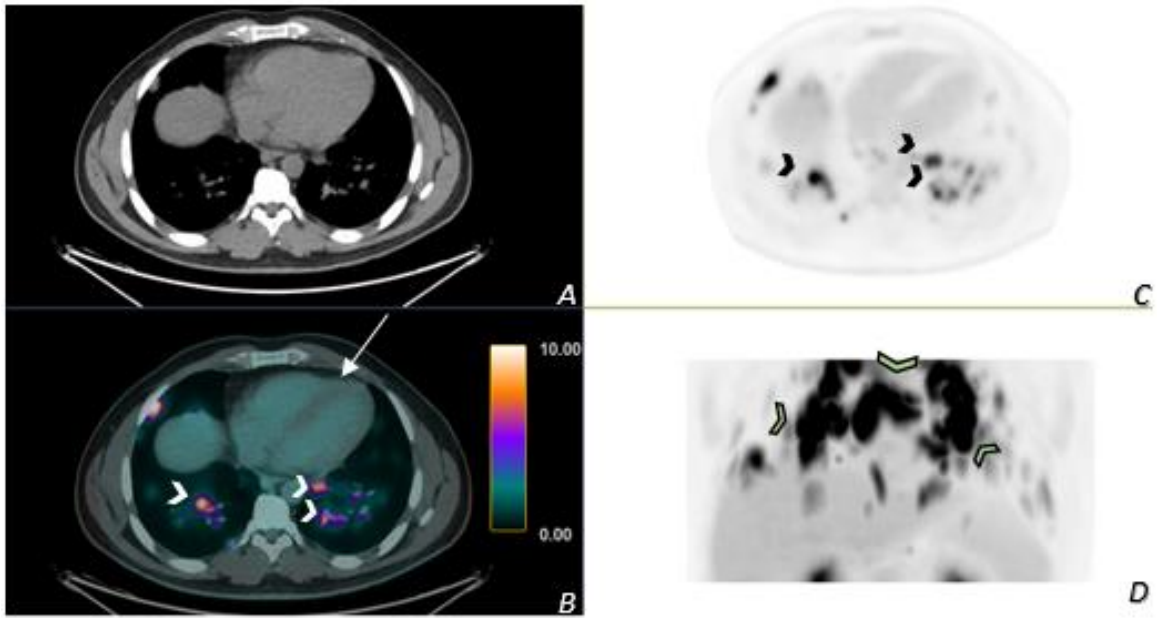

Figure 13

Figure 13: Successful suppression of the myocardial uptake in a patient without CS who received heparin and stuck to the dietary restrictions. The missing uptake (arrow) in the septum is in both panel B and C. Hilar and mediastinal lymph nodes and metabolically active lung nodes (arrowheads) are displayed in panels B, C and D, indicating sarcoidosis.

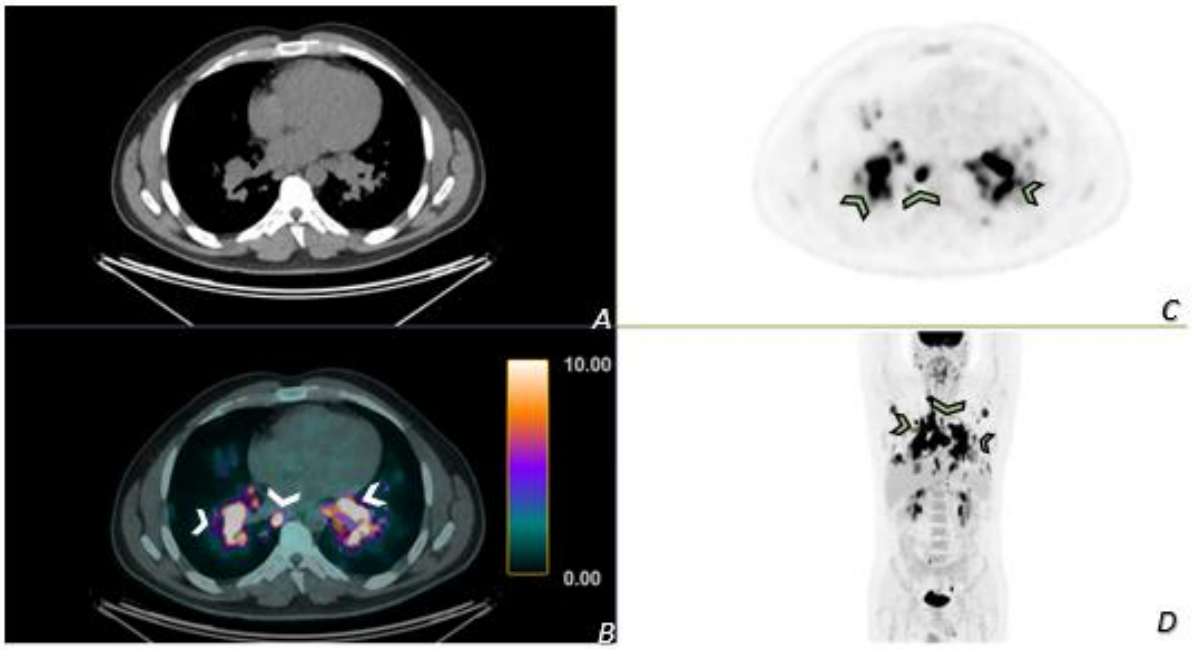

Figure 13a

Figure 13a: Strong uptake in the hilar/mediastinal lymph nodes and adjacent lung tissue (arrowheads) in the late phase PET scans (panel B, C, and D) indicating sarcoidosis, without cardiac involvement, as no uptake presents in the myocardium.

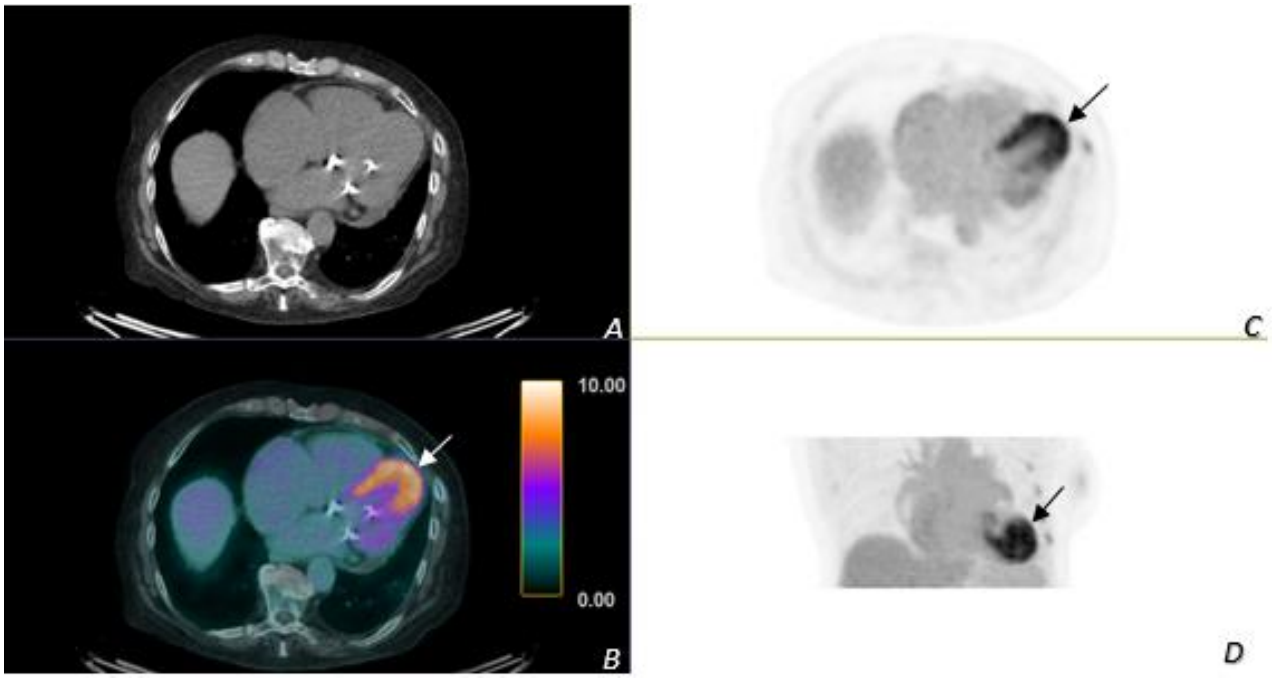

Figure 14

Figure 14: Strong myocardial uptake in the early phase in the left ventricle covering the whole apex, the anterior and septal wall (arrow) in panel B, C, and D. Patient was confirmed with CS, stuck to the dietary protocol and due to anticoagulation, received no heparin injection.

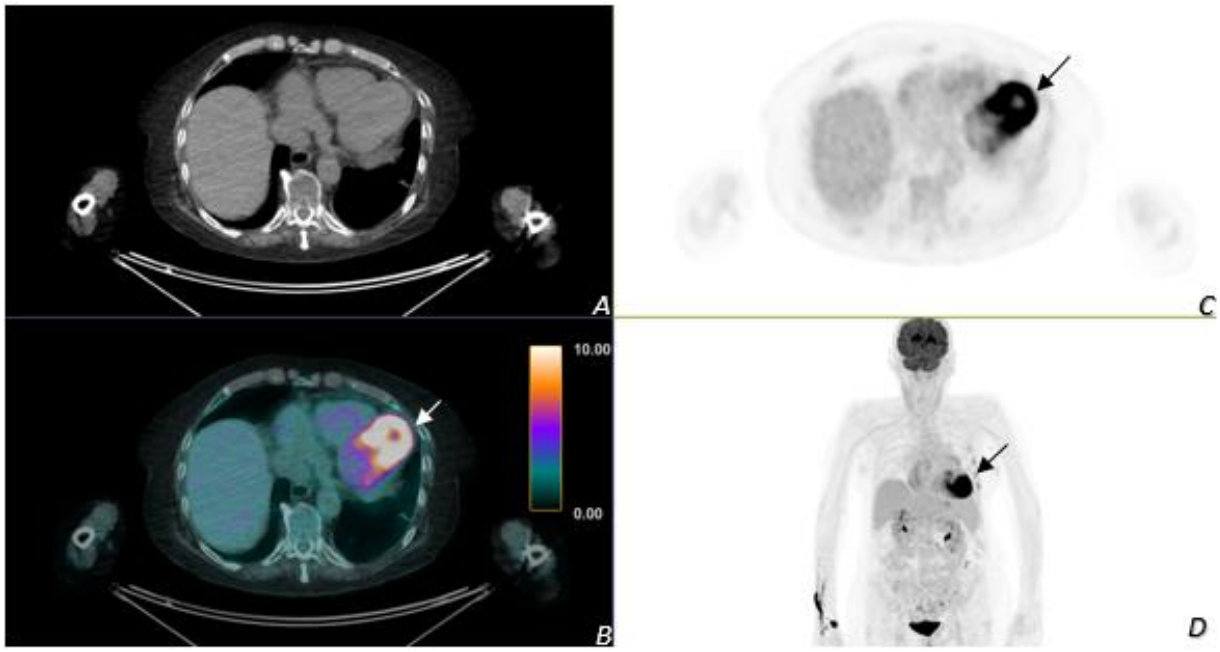

Figure 14a

Figure 14a: Same patient as in figure 14. The late acquisition shows the ongoing strong myocardial uptake (arrow) in panel B, C and D. No extra-cardiac involvement is present in the maximum intensity projection (panel D)

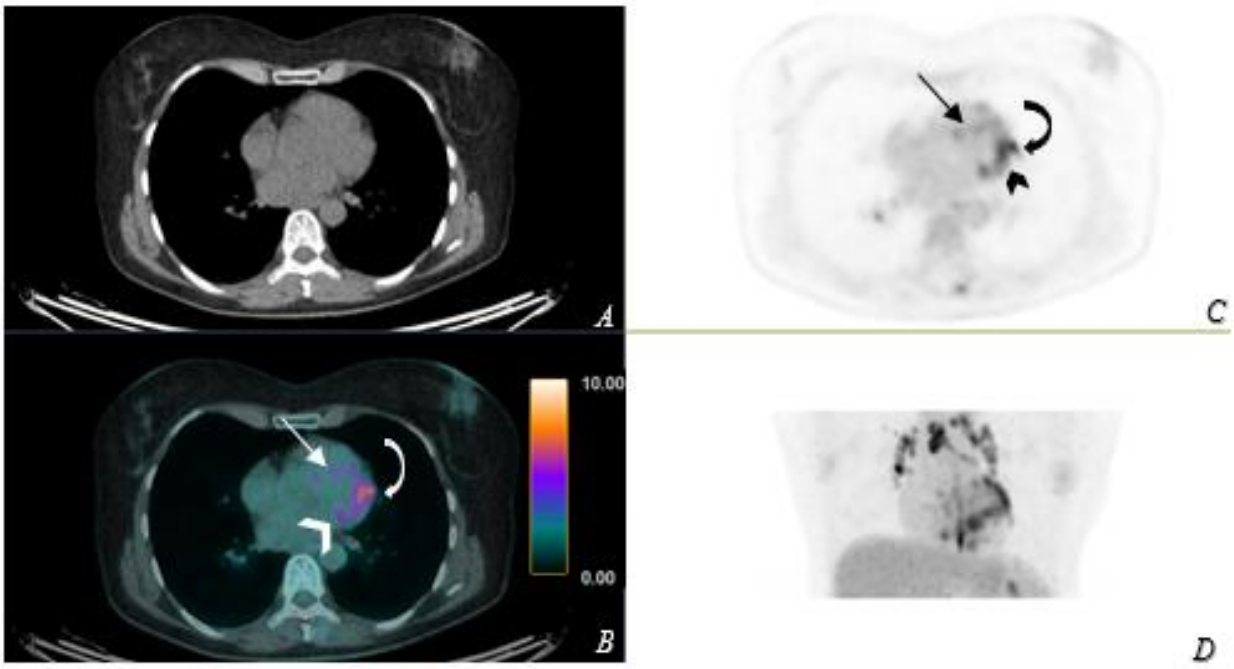

Figure 15

Figure 15: Myocardial uptake in a patient with CS, with both dietary preparations and heparin injection, in the early phase. In this case, the uptake intensity and the disseminated myocardial uptake pattern indicate CS with a high probability. In panel C and D uptake in the left ventricle in the apico-lateral wall (curved arrow) and in the anterolateral wall (arrowhead) and minimal activity in the intraventricular septum (arrow) is shown. Figure 15a, figure 15b and figure 15c are from the same patient as figure 15.

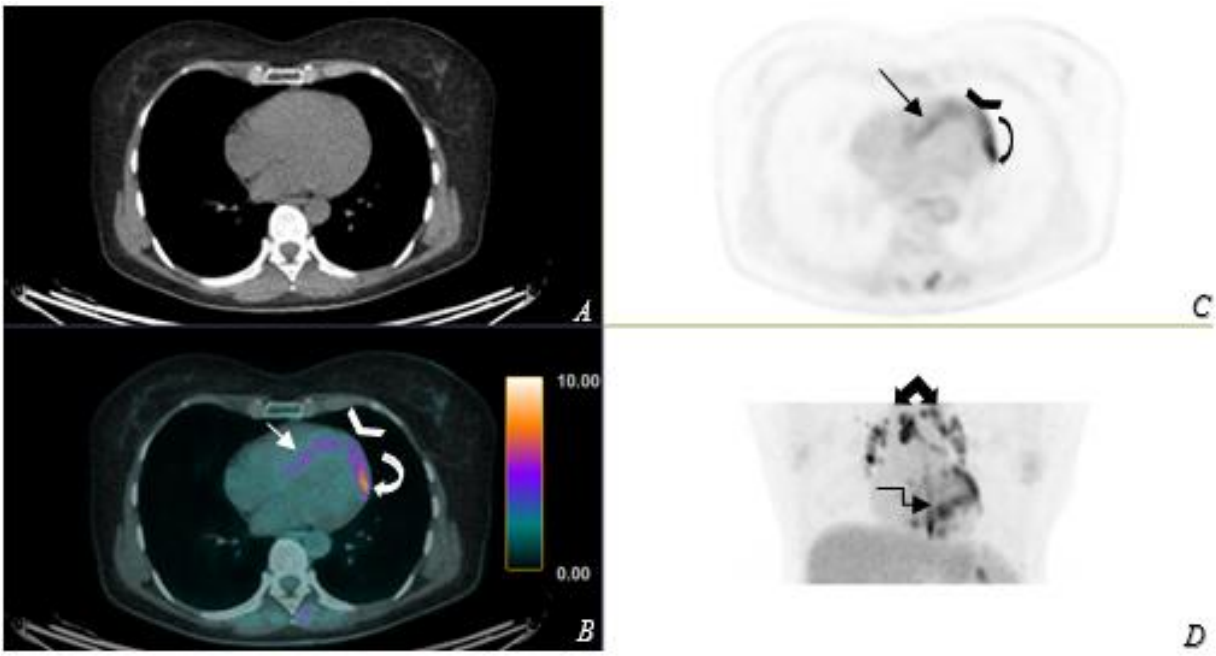

Figure 15a

Figure 15a: Pathological uptake in the early phase, in both panel B and C in the intraventricular septum (arrow) with an additional uptake in the apex (arrowhead) and the lateral wall (curved arrow) of the left ventricle. A strong uptake in the hilar/mediastinal lymph nodes presents in panel D (double-headed arrow), as well as the myocardial uptake (arrow with a step), suggesting sarcoidosis with cardiac involvement.

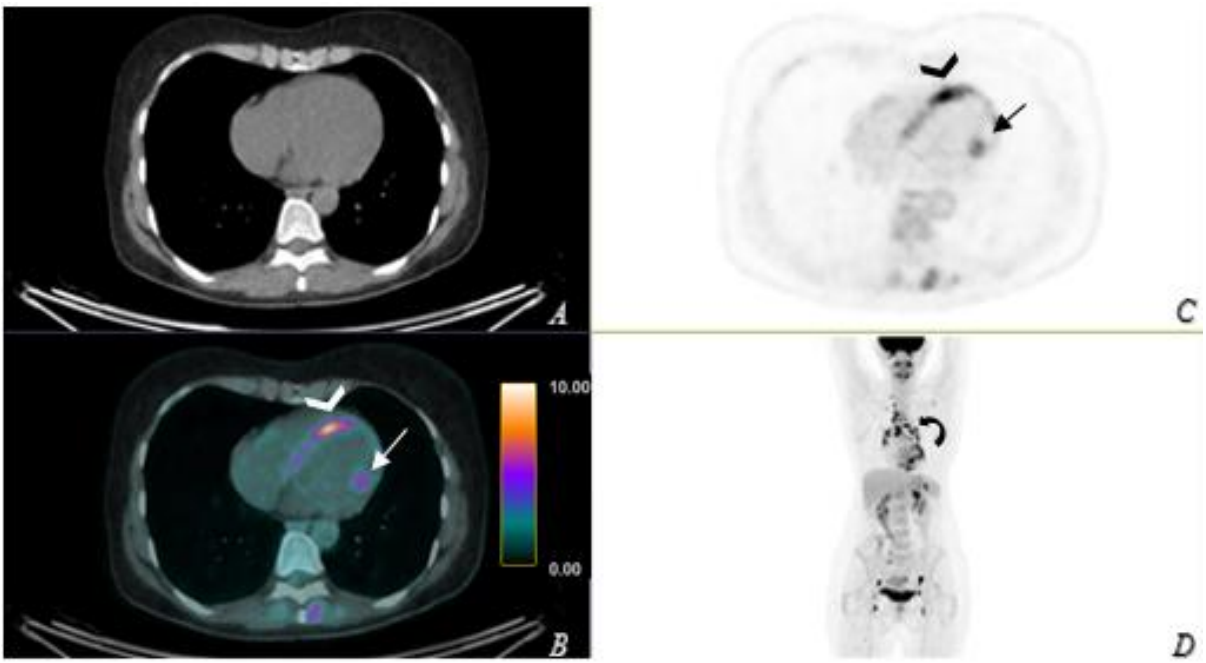

Figure 15b

Figure 15b: Late phase PET scans. Persistent myocardial uptake in the ventricular septum (arrowhead) in panel B and C, as well as small focal uptake (arrow) in the antero-lateral wall of the left ventricle. In panel D an elevated uptake in the hilar/mediastinal lymph nodes indicating sarcoidosis is shown (curved arrow).

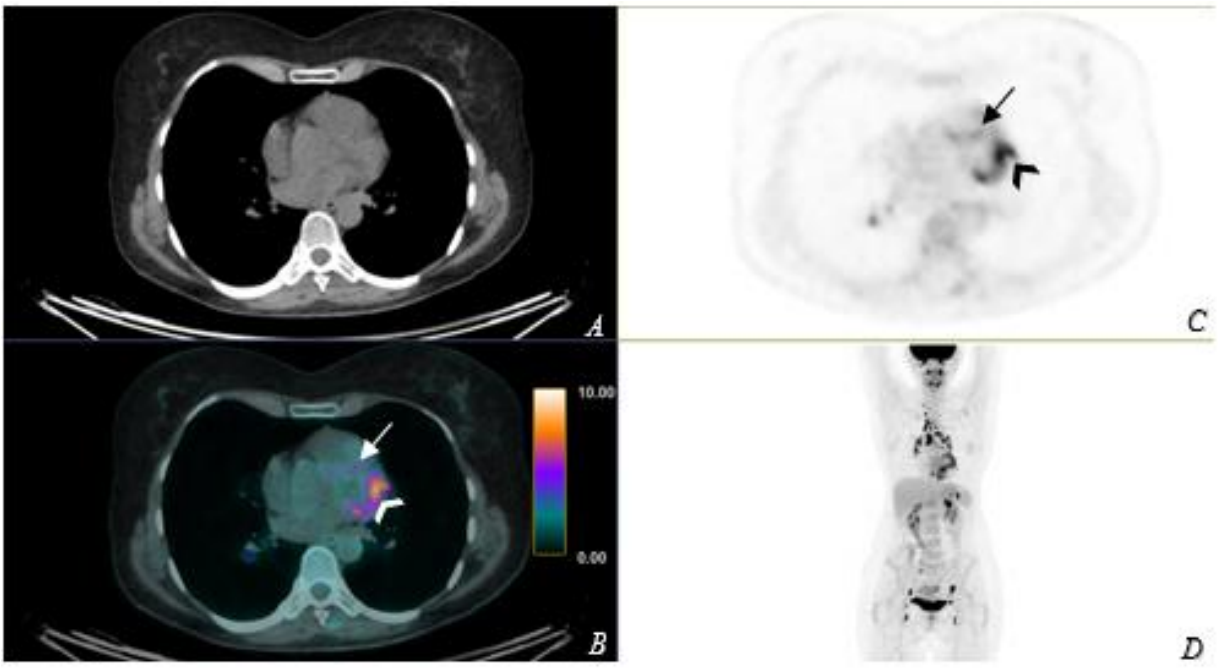

Figure 15c

Figure 15c: Myocardial uptake in the late phase (arrowhead) focusing on the left ventricle covering the lateral myocardial wall in panel B and C, while a small amount of activity is present in the septum (arrow). Maximum intensity projection in panel D shows lymph node involvement.

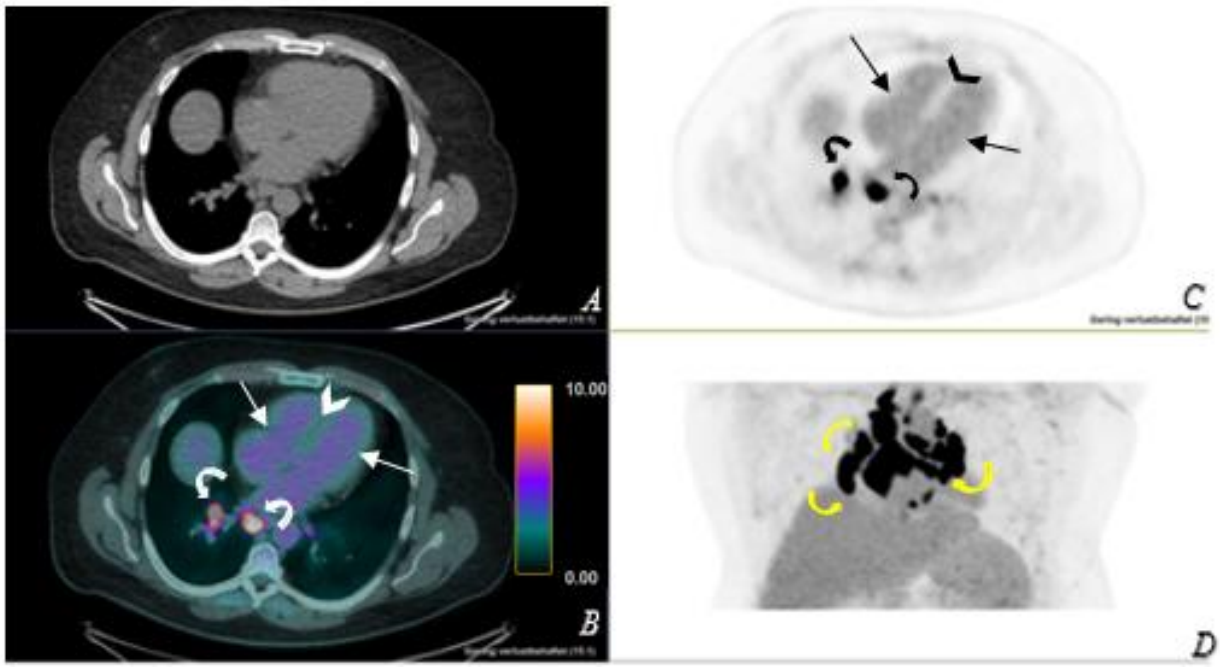

Figure 16

Figure 16: This patient stuck to the dietary restrictions and received a heparin injection. Based on the absent myocardial uptake pattern in the early phase, there is no indication of CS. Significant uptake in the blood pool in the heart (arrows) without septal involvement (arrowhead) both in panels B and C. Strong symmetrical uptake in hilar/mediastinal lymph nodes (curved arrows) seen in panels B, C, and D indicating sarcoidosis.

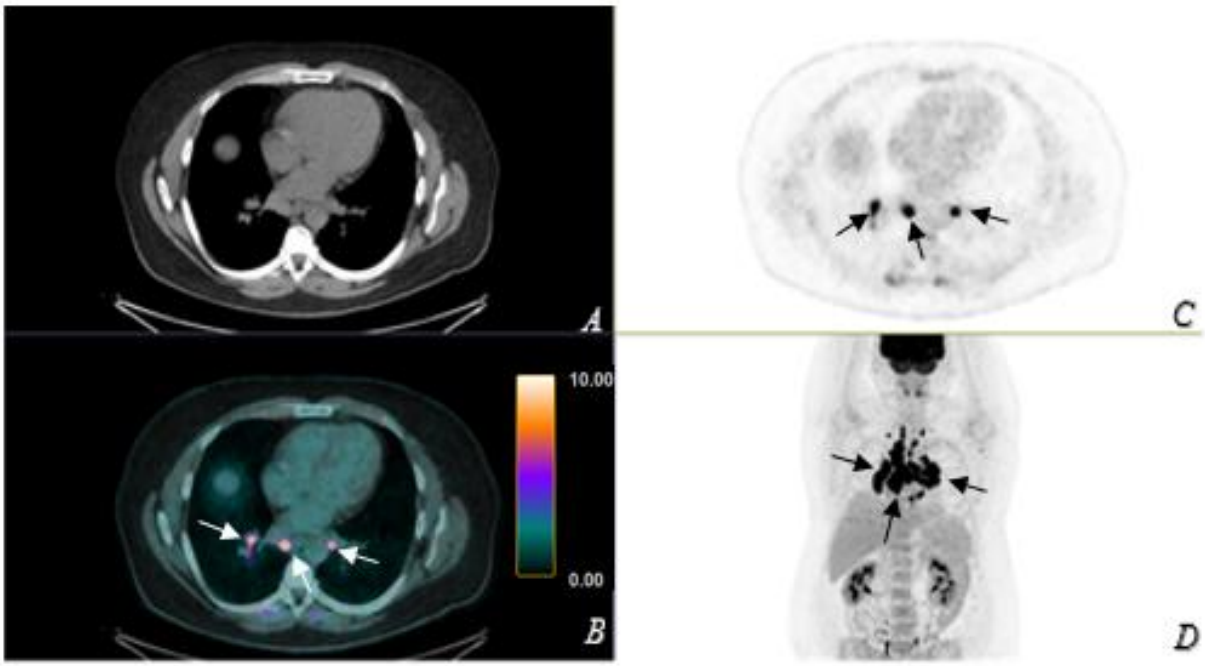

Figure 16a

Figure 16a: Same patient as in figure 16. The late phase acquisition shows a beneficial value in diagnosing CS. Less activity in the PET scans concerning the background activity. Nonetheless, there is an elevated symmetrical uptake in the grouped hilar/mediastinal lymph nodes indicating sarcoidosis (curved arrow) in panels B, C, and D.

This study was performed in accordance with the principles of the Declaration of Helsinki and its further amendments. Approval was granted by the Ethics Committee at the Medical University of Graz (EK-number: 35-471 ex 22/23). Being a retrospective study the need for written informed consent was waived.

3. Results / Findings

All patients received dual-staged [^{18}F]FDG PET/CT scans consisting of an early scan of the thorax performed 45 minutes p.i. (47.33 ± 4.57 [42.76;51.91] and late whole-body scan 90 minutes p.i. (92.00 ± 4.36 [87.64 to 96.36] p.i.). Patient characteristics can be found in table 1. All patients were evaluated by their [^{18}F]FDG PET/CT scans and CS diagnosis was based on these scans. This resulted in a group of [^{18}F]FDG PET/CT CS positive patients (n=15) and [^{18}F]FDG PET/CT CS negative patients (n=50).

Characteristic	PET positive patients (n=15)	PET negative patients (n=50)	P value
Mean Age (years)	52	55	0.3716
Sex ratio **Women, n** **Men, n**	 11 (73%) 4 (27%)	 21 (42%) 29 (58%)	
Mean weight (kg)	75.3	85.6	0.1542
Mean height (cm)	168	174.5	0.01807
Mean BMI	27	28	0.6205
Mean MBq of [18F]FDG	226.2	237.1	0.7208

Table 1 Descriptive statistics of the patient groups (BMI – body mass index).

Table 2 shows a variety of different parts of the heart affected with the uptake of [^{18}F]FDG. We observed the similarities and differences in the early and late images. In the early acquisition, as well as in the late acquisition the majority of affected areas showcased no change throughout the imaging procedure. The most involved area was the left ventricle 13/15 (86.7%). Other areas, such as the apex 7/15 (46.7%) and the right ventricle 6/15 (40%) were also affected in several patients. The right atrium 2/15 (13.3%) and the coronary sulcus 1/15 (6.7%) were affected even less than the prior locations, with the left atrium 0/15 coming dead last. Only in two areas differences between the early and late acquisition was observed.

These differences were found in two patients with one patient missing the lesion in the septum in the early phase as opposed to the late phase in which the lesion in the septum was detectable. The other patient did not express an uptake in the early acquisition in the papillary muscles as opposed to their later phase, where a lesion was found. This adds up to the affection of the septum from the early 10/15 (66.7%) in comparison to the late phase 11/15 (73.3%) and the papillary muscles in the early 3/15 (20%) to the late phase 4/15 (26.7%). There was one patient in this study, that had a broad uptake of [^{18}F]FDG in their heart in both phases, however there was a broad and sharp gap of no uptake in the left lateral wall of the myocardium, most likely due the implantation of a device into the myocardium years prior.

	Early		**Late**	
	N = 15	%	N = 15	%
Right atrium	2	13.3	2	13.3
Right ventricle	6	40.0	6	40.0
Left atrium	0	0	0	0
Left ventricle	13	86.7	13	86.7
Septum	10	66.7	11	73.3
Apex	7	46.7	7	46.7
Papillary muscles	3	20	4	26.7
Coronary sulcus	1	6.7	1	6.7

Table 2 Distribution locations in the heart.

In addition to the variety of different parts of the heart affected due to CS, a notable observation is the distribution pattern seen in patients with CS as visible in table 3. We differentiated either a multifocal or a focal distribution pattern and, in our case, we had a huge difference in those patterns. The multifocal pattern 11/15 (73.3%) was more often present than the focal pattern 4/15 (26.7%).

	N = 15	%
Multifocal	11 (2 ICS)	73.3
Focal	4 (3 ICS)	26.7

Table 3 Distribution pattern of [^{18}F]FDG.

As already stated above, sarcoidosis can affect a variety of different organs, sometimes a number of organs at the same time, as well as solely the heart, as table 4 shows. In our patient pool, involvement of sarcoidosis in different organs is seen in the lungs 5/15 (33.3%), hilar/mediastinal lymph nodes 7/15 (46.7%), extra thoracic lymph nodes 5/15 (33.3%), the spleen 2/15 (13.3%), the liver 1/15 (6.7%), the bones 1/15 (6.7%), and the skin 1/15 (6.7%). However, some patients presented with an ICS 5/15 (33.3%), as no other pathological uptake in other parts of the body could be seen. An interesting additional observation was the fact, that 3/4 (75%) patients with a focal uptake pattern had ICS, while in the bigger, multifocal uptake pattern group only 2/11 (18.2%) patients presented with ICS.
In the early images additional vasculitis in the thoracic aortic wall was only found in 1/15 (6.7%) patients, while in the late images 5/15 (33.3%) patients showcased vasculitis in the thoracic aortic wall due to lower physiological background uptake.

	N = 15	%
Solely the heart	5	33.3
Extra-thoracic lymph nodes	5	33.3
Mediastinal lymph nodes	7	46.7
Lungs	5	33.3
Liver	1	6.7
Spleen	2	13.3
Skin	1	6.7
Bones	1	6.7

Table 4 Location of non-caseating granulomas in other parts of the body.

Table 5 shows that out of 15/65 PET positive patients, 8/15 received a biopsy and the remaining 7/15 patients did not. Out of the 8/15 patients only 2/15 (13.3%) had a positive finding in their biopsy while the other 6/15 (40%) had a negative outcome. This means, that solely 2/15 patients had a histological verified CS.
Out of the 50/65 PET negative patients, 12/50 (24%) patients received a biopsy and 38/50 (76%) patients did not undergo a biopsy. None of the 12 patients that underwent a biopsy were considered positive for CS.

	N = 15	%	N = 50	%
Positive biopsy	2	13.3	0	0
Negative biopsy	6	40	12	24
No biopsy performed	7	46.7	38	76

Table 5 Biopsy in the patient collective.

Table 6 shows four different parameters for the entirety of our positive CS patient collective, as well as the data of the patients based on their anticoagulation. Beginning with the myocardial SUVmax average from the early images there is a clear trend throughout the patient collective. The averages of the upper four categories in the complete patient pool (n=15) were slightly higher than those of the patients with heparin and lower than the averages of the patients with another form of anticoagulation. The patients, which received the heparin, showcased the lowest average myocardial SUVmax with a value of 6.43, while the patients who did not receive heparin, had a staggering average value of 8.88. The same circumstance is present in the average myocardial SUVmax from the late images, as the patients with heparin had an average myocardial SUVmax of 8.04, whilst the patients without heparin had an average myocardial SUVmax of 11.91. However, another factor that has to be mentioned is the tissue to blood ratio (TBR), defined as the ratio of specific [^{18}F]FDG uptake in the myocardium compared to the uptake of the aortic arch. A low TBR value shows that the suppression of physiological myocardial uptake is successful, as only pathological uptake should show up in myocardium. Patients with heparin had a lower TBR (3.29) than the patients without heparin (4.80). As generally accepted according to the pathophysiology of [^{18}F]FDG active lesion constantly accumulate over time. Therefore we found higher SUVmax in the late scans. All of our patients had the same uptake pattern in

their [^{18}F]FDG PET/CT scan, in both their early and late images. The mentioned uptake is in accordance with CS typical lesions. We found a rise of 127% in the average myocardial SUVmax uptake between the early and late scans in our PET-positive patient collective. Additionally, there was a rise of 125% in the average myocardial SUVmax uptake in patients with heparin and 134% in patients without heparin in between the early and late scans.

Characteristic	PET positive patients (n=15)	Patients with heparin 12/15	Patients without heparin 3/15
Myocardial SUVmax (early) average (Confidence level of 95%)	6.92 ± 1.24 [5.69;8.16]	6.43 ± 1.39 [5.04;7.82]	8.88 ± 1.21 [7.67;10.09]
Myocardial SUVmax (late) average (Confidence level of 95%)	8.81 ± 1.69 [7.12;10.50]	8.04 ± 1.63 [6.41;9.67]	11.91 ± 4.29 [7.62;16.2]
TBR average (Confidence level of 95%)	3.60 ± 0.64 [2.96;4.24]	3.29 ± 0.65 [2.64;3.94]	4.80 ± 1.26 [3.54;6.06]
Aortic arch SUVmax average (Confidence level of 95%)	2.46 ± 0.24 [2.22;2.70]	2.45 ± 0.29 [2.16;2.74]	2.47 ± 0.39 [2.09;2.86]

Table 6 Results of semi-quantitative parameters for the groups (SUVmax – maximum standard uptake value, TBR – Tissue to blood ratio.

4. Discussion

The cardiac involvement in sarcoidosis poses a life-threatening circumstance, affecting more people than originally anticipated (1–9). A variety of recommendations exist showcasing several diagnostic approaches for diagnosing CS like the EMB, ECG, TTE, CMR and the PET/CT for an instance. No standardized preparation protocol for [^{18}F]FDG PET/CT imaging in CS have been established yet, although several proposals have been suggested (6,16,30).
Sarcoidosis is characterized by infiltration of inflammatory cells including macrophages and lymphocytes resulting in high glucose utilization. [^{18}F]FDG PET/CT therefore represents a viable diagnostic tool in nuclear medicine, although detecting the difference between a possible diffuse physiological myocardial uptake from a pathological myocardial uptake remains challenging (1,3,4,10,19,21–29,32).

Although extensive research has been carried out on examination tools and protocols on CS, no identical comparison ground is available for this study. Different aspects for preparation and execution, like varying acquisition times, different time ranges for fasting and dieting, as well as the usage of i.v. heparin, have not been investigated abundantly (33–37).
All of these factors combined to maximize the effects of physiological suppression have also not been considered yet. Following this state, this retrospective study is one of the first conducting and differentiating dual-staged [^{18}F]FDG PET/CT scans combined with both heparin usage and diet restrictions in diagnosing CS.

This study mainly focused on the value of a dual-staged [^{18}F]FDG PET/CT acquisition. The acquired scans showcased the differences of the early and late images in diagnosing patients with CS. As expected, major increase of the average myocardial SUVmax between the early and late scans was present. All of our patients (n=15) had CS-like uptake in both their early as well as their late [^{18}F]FDG PET/CT scans that was sufficient enough for diagnosing. Nonetheless, there were two patients, which showed an additional lesion in the late scans. One of the patients showed an additional lesion in the septum in the later image, while the other patient only showed an additional lesion in the papillary muscles in the late scans, visually distinguishable from possible physiological myocardial uptake.

Manabe et al. described in their work the difference between the myocardial SUVmax from early and late acquisition. Their patients only stuck to an 18-hour diet prior to their scans without the usage of heparin. The scans showed that 21/23 (91.3%) patients had early uptake indicating CS in their scans, while 2/23 (8.7%) patients did not. In the late scans, 23/23 (100%) patients had pathological myocardial uptake indicating CS. These findings are in accordance with our findings.

We also found an increased uptake in late scans with a rise of 127% in the average myocardial SUVmax (from an average rise of 6.92 ± 1.24 in the early scans to an average of 8.81 ± 1.69 in the late scans). This increase leads to a higher degree of certainty in difficult cases, especially in cases when findings in the early images are equivocal.
Manabe et al. found an average rise in myocardial SUVmax between the early and late images of 145%, similar to our study. Both Manabe's and our results indicate a better visual assessment of CS in [^{18}F]FDG PET/CT scans with delayed acquisition time (38).

In addition, we also found out, patients who received heparin had a rise of 125% in the average myocardial SUVmax (from an average rise of 6.43 in the early scans to an average of 8.04 in the late scans) and a rise of myocardial SUVmax of 134% (from an average rise of 8.88 in the early scans, to an average of 11.91 in the late scan) in the patients without heparin intake. However we were not able to prove any statistical significance, as this patient collective was too small.

With the later acquisition, the activity of CS usually increases resulting in a higher degree of certainty when diagnosing. The late whole-body acquisition is beneficial in terms of detecting extra-cardiac lesions, which were presented in the majority of our patient collective. Two additional cardiac lesions also only showed up in later images, which can be of therapeutic and diagnostic value.
From an economic point of view, the adaption of a single-staged, late image acquisition would pose major benefits. Dual-staged protocol pose more stress for immobile and frail patients as well as the staff. This also leads to elongated waiting period for other patients waiting for their PET/CT scans, and further additional cost due to the unstoppable radionuclide decay. Dual-staged protocol call for time buffers, which may minimize the possible maximum of PET/CT appointments each day.

Dual-staged image acquisition protocols are useful in numerous other examinations based on a variety of studies.

Chan et al. showcased the efficiency of a dual-staged imaging process in 53 patients with various tumors. There was a significant increase of the sensitivity in the detection of malignancy, with a 94% detection rate in the late image as opposed to the early image with a rate of 77% (39).

Another study by Bermejo et al., looked at the value of a dual-staged imaging in diagnosing endocarditis. They found that a delayed acquisition was helpful in certain cases with inconclusive imaging results (40).

In a study by Tian et al., a dual-staged [^{18}F]FDG PET/CT acquisition protocol was applied in patients with unclear bone lesions. This study showcased, that the dual-timed acquisition can be of great use in terms of differentiating between malignant and benign bone lesions, as it has the ability to show SUV values of both the early and late scans to be compared (41).

Costantini et al. showcased the advantage of a dual-time point [^{18}F]FDG PET/CT in patients with pediatric tumors. The data showed a grave rise of the average SUV from 7.3 ± 1.2 to 10.9 ± 2.7 in malignant tumors, while the average SUV in benign tumors ranged from 4.5 ± 0.8 to 4.2 ± 1.0, showing that with the adaption of a later acquisition, the differentiation of malignancy can be done with a higher degree of certainty (42).

The dual-staged [^{18}F]FDG PET/CT was used as an examination option, in a study conducted by Zytoon et al., for differentiating between invasive and non-invasive breast cancers. The data of this study showed an elevated sensitivity in terms of finding cancers in tissue with a high degree of density, as well as cancers smaller than 1 cm, if an added late image acquisition was added (43).

In order to receive the best possible results while scanning, sticking to a regulated diet plays a vital role in the suppression of physiological [^{18}F]FDG uptake in the myocardium (23). Nevertheless, the uptake suppression, due to a regulated diet, may not work out in about 20% of cases (33).

Our protocol includes dietary restrictions lasting for 48 hours with the exclusion of carbohydrate products, only allowing a diet consisting of protein and fat. Included in this preparation is a 12 hour long fast, which only allows the consumption of water and unsweetened beverages prior to the scans. These restrictions showed a strong suppression of physiological [^{18}F]FDG uptake in the myocardium. Previous studies with different dietary

preparations support this circumstance, however with different approaches and results (34,35).
Özütemiz et al. presented in their study one group sticking to a diet for 24 hours with an additional fast of 6 hours prior to scanning and the other group following a fast lasting for 18 hours. Both groups showed a high margin of failed myocardial uptake suppression. The first group had 23.4% failed myocardial uptake suppression and the other group even showed 25% of failed myocardial uptake suppression (35).

Balink et al. investigated the difference in myocardial [^{18}F]FDG uptake between a group without a diet and another group with a diet lasting for 24 hours prior to scanning. This resulted in a much higher uptake suppression of [^{18}F]FDG in the myocardium in the group with a diet with 68% of all the participants having a complete uptake suppression. On the other hand, the group without a diet only had 15% of all their participants showing a complete uptake suppression (34).
This same effect was seen in a study by Özütemiz et al., which compared three groups with different dietary orders. The group with the longest diet (approximately 72 hour long fast) showed the highest uptake suppression with 96.9% of all the participants showcasing a complete uptake suppression, unlike the group with the shortest diet (24 hour long fast), which only had 68.1% of the participants with a complete uptake suppression. This supports the hypothesis of beneficial effects of dietary restrictions for diagnosing CS with a higher degree of certainty (35).

In our study, we did not have a control group of patients without a diet, so we could not pose such a comparison. The main difference our study had was the inclusion of patients with suspected active CS, as the other two studies had other patient collectives (34,35).
Additionally, our protocol has a regulated dietary basis, excluding certain aliments that could falsify the results. This was not as regulated in the study by Balink et al. as they did not directly exclude nourishments like fruits, honey, fermented and whole milk products (34).

Due to this circumstance, Madamanchi et al. showed the value of serum beta-hydroxybutyrate, which can ultimately help differentiate the failed myocardial uptake suppression and extract pathological scans (33). In our study we did not draw blood to check the beta-hydroxybutyrate levels.

The usage of heparin is known to elevate FFA by activating the lipase, thus increasing metabolism based on fatty acids in healthy myocardial tissue (22,26).
In our study we had 12/15 patients that received heparin and only 3/15 patients that received another form of anticoagulation, like Rivaroxaban, Apixaban and Phenprocoumon. This patient collective was too small to create two subgroups and compare the patients with heparin and those without in order to receive scientifical significant data based on their SUVmax average. Nonetheless, certain differences were found that would produce important data in bigger patient collectives. The differences we found, showed that the patients with heparin had a smaller SUVmax average of 6.43 ± 1.39, whilst the patients with other forms of anticoagulation had 8.88 ± 1.21, this was also detectable visually.
In the late images the SUVmax average of those with heparin was 8.04 ± 1.63, while patients without heparin had a much higher value of 11.91 ± 4.29, which shows that the patients with heparin had a weaker [^{18}F]FDG uptake in the PET/CT scans. This may indicate that a stronger uptake suppression took place in the patients with heparin intake.
This circumstance is important to consider, as a number of studies dismiss the usage of i.v. heparin and mainly focus on different preparation protocols (34,35).

A study performed by Manabe et al., showed the benefits of adding i.v. heparin to the protocol combined with different length diets in two groups to suppress the physiological myocardial uptake of [^{18}F]FDG in PET/CT scans. This study showed that the highest uptake suppression was found in the group with a low-carbohydrate diet and a fasting period lasting more than 18 hours. The diffuse uptake pattern, which was seen as a physiological mechanism, was nonexistent in the group with the fast lasting for more than 18 hours, unlike in the other group, which only had a fast lasting for 6 hours without any other dietary restriction. This group showed missing myocardial uptake suppression in 27.6% of all participants. This may indicate that a longer diet combined with the usage of heparin may suppress the physiological uptake by an enormous margin, making the differentiation of physiological and pathological uptake patterns more visible (36).
This effect can also be seen in our study as we differentiated between a bolus of heparin and other blood thinners taken, although not as notable as in the study above, however this may be due to other blood thinners having a similar, but less significant effect as heparin. Our

study also included a diet lasting for 48 hours, so the comparison of our study and this one is quite reasonable.
Nonetheless, this study focused on a single scan after 60 minutes and different diet lengths with heparin usage, while our groups had a dual-staged [^{18}F]FDG PET/CT acquisition and all of our PET positive patients had the same dietary restrictions prior to scanning (36).
This same circumstance can be seen in a study by Sekiguchi et al. showcasing the suppression of physiological uptake of [^{18}F]FDG in the myocardium compared to the liver. They compared three groups with different dietary restrictions with only two groups receiving a heparin injection. The group with the strongest uptake suppression had the longest fast and also received a heparin injection, unlike the group without heparin and a short diet, which displayed a weak physiological suppression. These results are indicating that the usage of heparin with a diet helps suppressing physiological uptake in the myocardium by a big margin, making it easier to differentiate between healthy and CS affected myocardium (37).
This could be visually detected in our study as well. Patients, that received heparin, presented with a lower myocardial uptake average in both early and late images than patients who did not receive heparin due to their already existing anticoagulation.

In this thesis, we only focused on the nuclear medical imaging to detect CS, not on other modalities like the EMB. However, the EMB is the first fundamental examination tool for CS. A study by Uemura et al. found, that the diagnosis of CS solely through EMB was tied to a high grade of uncertainty. Out of 105 specimens only 5 patients showed positive CS cases with granulomatous inflammations. Thus, diagnosing CS merely with EMBs shows underwhelming results, even if multiple biopsies succeeded in one patient (44).
Concerning CS, the EMB ranks rather low with its success of 20-30% of cases turning PET positive in actual sick patients, due to the different distribution patterns CS can produce. The variety in those patterns, even if there are granulomas in the cardiac tissue, can ultimately turn negative (13).

In comparison with post-mortem autopsies, diagnosing CS had a higher success rate than in-vivo (37). The reasoning for a lower sensibility may be tied to either larger sample size or the disease not being in such an established state to confirm CS histologically (44).

Independently, a study by Simonen et al. focused on collecting samples from the mediastinal lymph nodes guided by [^{18}F]FDG PET scans. There was a higher occurrence of biopsy proven CS than in previous studies that did not include [^{18}F]FDG PET/CT as a navigation tool. They did not extract the biopsies from the heart; however they showcased the high accumulation rate of NCG in other tissues (45).

In our study, we did not focus on EMBs, however some were performed in addition to PET/CT, nonetheless. From our PET positive patient pool (n=15), 8/15 (53.3%) patients did undergo a biopsy, whilst the other 7/15 (46.7%) patients did not undergo such a procedure. Out of the patients with a biopsy, only 2/15 (13.3%) confirmed CS. In the remaining 6/15 (40%) patients, the EMB showed equivocal results, leading to only [^{18}F]FDG PET/CT confirmed CS. This circumstance may alone show the importance of [^{18}F]FDG PET/CT scans in order to properly diagnose CS, although our study population was not broad enough to make such an assumption. In those six patients with equivocal EMBs a variety of factors should be mentioned. For one, if there is no imaging guidance in the procedure of the biopsy, samples free from NCG can possibly be extracted from a sick heart, due to the nature of the distribution pattern of CS, which can be unpredictable leading to false-negative results. Other reasons for equivocal results can involve the process after extraction with incorrect storing. With the certainty of the location of specific lesions, an EMB can be performed with the guidance of PET/CT. This examination comes with the benefit of being as non-invasive as possible which can ultimately lead to an even higher degree of certainty in diagnosing, with creating as little damage as possible.

Critical reflection and implications

This study has a few limitations. CS is a rare and seldom recognized illness, and it is not as common in the Austrian population as in other countries like Finland or Japan. Due to its complex pathophysiological background it is even harder to detect solely through symptoms, so a majority of patients do not get sent to [^{18}F]FDG PET/CT scanning. Moreover, this is a monocentric study. Furthermore, due to our strictly defined inclusion and exclusion criteria, we only included a small study population as those examinations in our analysis were performed for staging which could differ in follow-up examination according to alternating disease burden. We assumed that all patients stuck to dietary restrictions.

Conclusion

Early acquisition of the thorax in the dual-staged imaging protocol added no additional information for diagnosing cardiac sarcoidosis. The late images alone proofed to be sufficient, due to the higher pathological tracer uptake and higher tissue-to-blood ratio in the suspicious myocardial lesions for CS. Late scans were also able to show additional sarcoidosis related lesions in the whole-body, as opposed to the smaller image field of the early scans, which only had their field of view on the thorax. Additionally, the usage of heparin prior to scanning showed a better suppression of physiological [^{18}F]FDG uptake as opposed to patients without the usage of heparin. Due to the data from this study, there is no additional value in performing the dual-staged protocol, thus not adding an early scan is justified in the diagnosis of CS.

References

1. Lehtonen J, Uusitalo V, Pöyhönen P, Mäyränpää MI, Kupari M. Cardiac sarcoidosis: phenotypes, diagnosis, treatment, and prognosis. European Heart Journal [Internet]. 2023 Mar 16;44(17):1495–510. Available from: https://doi.org/10.1093/eurheartj/ehad067
2. Baughman RP, Lower EE. Who Dies from Sarcoidosis and Why? American Journal of Respiratory and Critical Care Medicine [Internet]. 2011 Jun 1;183(11):1446–7. Available from: https://doi.org/10.1164/rccm.201103-0409ed
3. Lagana SM, Parwani AV, Nichols L. Cardiac Sarcoidosis: A Pathology-Focused Review. Archives of Pathology & Laboratory Medicine [Internet]. 2010 Jul 1;134(7):1039–46. Available from: https://doi.org/10.5858/2009-0274-ra.1
4. Birnie DH, Nery PB, Ha ACT, Beanlands RS. Cardiac sarcoidosis. Journal of the American College of Cardiology [Internet]. 2016 Jul 1;68(4):411–21. Available from: https://doi.org/10.1016/j.jacc.2016.03.605
5. Terasaki F, Azuma A, Anzai T, Ishizaka N, Ishida Y, Isobe M, et al. JCS 2016 Guideline on Diagnosis and Treatment of Cardiac Sarcoidosis ― Digest Version ―. Circulation Journal [Internet]. 2019 Oct 25;83(11):2329–88. Available from: https://www.jstage.jst.go.jp/article/circj/83/11/83_CJ-19-0508/_html/-char/en
6. Mathai SV, Patel SR, Jorde UP, Rochlani Y. Epidemiology, pathogenesis, and diagnosis of cardiac sarcoidosis. Methodist DeBakey Cardiovascular Journal [Internet]. 2022 Jan 1;18(2):78–93. Available from: https://doi.org/10.14797/mdcvj.1057
7. Kandolin R, Lehtonen J, Airaksinen J, Vihinen T, Miettinen H, Ylitalo K, et al. Cardiac sarcoidosis. Circulation [Internet]. 2015 Feb 17;131(7):624–32. Available from: https://doi.org/10.1161/circulationaha.114.011522
8. Isobe M, Tezuka D. Isolated cardiac sarcoidosis: Clinical characteristics, diagnosis and treatment. International Journal of Cardiology [Internet]. 2015 Mar 1;182:132–40. Available from: https://www.sciencedirect.com/science/article/pii/S0167527314024784
9. Greulich S, Deluigi CC, Gloekler S, Wahl A, Zürn C, Krämer U, et al. CMR imaging predicts death and other adverse events in suspected cardiac sarcoidosis. JACC: Cardiovascular Imaging [Internet]. 2013 Apr 1;6(4):501–11. Available from: https://doi.org/10.1016/j.jcmg.2012.10.021
10. Chen ES, Moller DR. Etiologies of Sarcoidosis. Clin Rev Allergy Immunol. August 2015;49(1):6–18.

11. Chen ES, Möller DR. Etiologies of sarcoidosis. Clinical Reviews in Allergy & Immunology [Internet]. 2015 Mar 15;49(1):6–18. Available from: https://doi.org/10.1007/s12016-015-8481-z

12. Kurmann R, Mankad S, Mankad R. Echocardiography in sarcoidosis. Current Cardiology Reports [Internet]. 2018 Sep 26;20(11). Available from: https://doi.org/10.1007/s11886-018-1065-9

13. Ahmed T. Endomyocardial biopsy [Internet]. StatPearls - NCBI Bookshelf. 2023. Available from: https://www.ncbi.nlm.nih.gov/books/NBK557597/

Ahmed T, Goyal A. Endomyocardial Biopsy. [Updated 2023 May 8]. In: StatPearls [Internet]. Treasure Island (FL): StatPearls Publishing; 2023 Jan-. Available from: https://www.ncbi.nlm.nih.gov/books/NBK557597/

Accessed June, 2023

14. Behrends J, Bischofberger J, Deutzmann R, Ehmke H, Frings S, Grissmer S et al. Physiologie [Internet]. 2017. 3rd edition. Stuttgart (GER): Georg Thieme Verlag. Chapter 4, Herz [cited 2023 Nov 17th]. Available from: DOI 10.1055/b-004-132217

15. Willy K, Dechering DG, Reinke F, Bögeholz N, Frommeyer G, Eckardt L. The ECG in sarcoidosis – a marker of cardiac involvement? Current evidence and clinical implications. Journal of Cardiology [Internet]. 2021 Feb 1;77(2):154–9. Available from: https://doi.org/10.1016/j.jjcc.2020.07.006

16. Skowasch D, Gaertner F, Marx N, Meder B, Müller-Quernheim J, Pfeifer M, et al. Diagnostik und Therapie der kardialen Sarkoidose. Der Kardiologe [Internet]. 2019 Dec 20;14(1):14–25. Available from: https://doi.org/10.1007/s12181-019-00359-y

17. Tadić M, Cuspidi C, Saeed S, Milojević B, Milojevic IG. The role of cardiac magnetic resonance in diagnosis of cardiac sarcoidosis. Heart Failure Reviews [Internet]. 2020 Oct 6;26(3):653–60. Available from: https://doi.org/10.1007/s10741-020-10035-z

18. Kiko T, Yoshihisa A, Kanno Y, Yokokawa T, Abe S, Miyata-Tatsumi M, et al. A Multiple Biomarker Approach in Patients with Cardiac Sarcoidosis. International Heart Journal [Internet]. 2018 Sep 1;59(5):996–1001. Available from: https://www.jstage.jst.go.jp/article/ihj/59/5/59_17-695/_pdf/-char/en

19. Lopci E, Hicks RJ, Dimitrakopoulou-Strauß A, Dercle L, Iravani A, Seban RD, et al. Joint EANM/SNMMI/ANZSNM practice guidelines/procedure standards on recommended use of [18F]FDG PET/CT imaging during immunomodulatory treatments in patients with

solid tumors version 1.0. European Journal of Nuclear Medicine and Molecular Imaging [Internet]. 2022 Apr 4;49(7):2323–41. Available from: https://doi.org/10.1007/s00259-022-05780-2

20. Stegger L, Eschner W. Messtechnik. In: Dietlein M, Kopka K, Schmidt M, editors. Nuklearmedizin Basiswissen und klinische Anwendung. 8th edition. Stuttgart (GER): Schattauer GmbH; 2017. p.82-107.

21. Boellaard R, Delgado-Bolton R, Oyen WJG, Giammarile F, Tatsch K, Eschner W, et al. FDG PET/CT: EANM procedure guidelines for tumour imaging: version 2.0. European Journal of Nuclear Medicine and Molecular Imaging [Internet]. 2014 Dec 2;42(2):328–54. Available from: https://doi.org/10.1007/s00259-014-2961-x

22. Armoni M, Harel C, Bar-Yoseph F, Milo S, Karnieli E. Free Fatty Acids Repress the GLUT4 Gene Expression in Cardiac Muscle via Novel Response Elements. Journal of Biological Chemistry [Internet]. 2005 Oct 14;280(41):34786–95. Available from: https://doi.org/10.1074/jbc.m502740200

23. Minamimoto R. Series of myocardial FDG uptake requiring considerations of myocardial abnormalities in FDG-PET/CT. Japanese Journal of Radiology [Internet]. 2021 Jan 31;39(6):540–57. Available from: https://doi.org/10.1007/s11604-021-01097-6

24. Randle PJ, Garland PB, Hales CN, Newsholme EA. THE GLUCOSE FATTY-ACID CYCLE ITS ROLE IN INSULIN SENSITIVITY AND THE METABOLIC DISTURBANCES OF DIABETES MELLITUS. The Lancet [Internet]. 1963 Apr 13;281(7285):785–9. Available from: https://www.sciencedirect.com/science/article/abs/pii/S0140673663915009

25. Metser U, Even-Sapir E. Increased 18F-Fluorodeoxyglucose Uptake in Benign, Nonphysiologic Lesions Found on Whole-Body Positron Emission Tomography/Computed Tomography (PET/CT): Accumulated Data From Four Years of Experience With PET/CT. Seminars in Nuclear Medicine [Internet]. 2007 May 1;37(3):206–22. Available from: https://doi.org/10.1053/j.semnuclmed.2007.01.001

26. Kumita S, Yoshinaga K, Miyagawa M, Momose M, Kiso K, Kasai T, et al. Recommendations for 18F-fluorodeoxyglucose positron emission tomography imaging for diagnosis of cardiac sarcoidosis—2018 update: Japanese Society of Nuclear Cardiology recommendations. Journal of Nuclear Cardiology [Internet]. 2019 Aug 1;26(4):1414–33. Available from: https://doi.org/10.1007/s12350-019-01755-3

27. Chareonthaitawee P, Beanlands RS, Chen W, Dorbala S, Miller EA, Murthy VL, et al. Joint SNMMI–ASNC expert consensus document on the role of 18F-FDG PET/CT in cardiac sarcoid detection and therapy monitoring. Journal of Nuclear Cardiology [Internet]. 2017 Oct 1;24(5):1741–58. Available from: https://doi.org/10.1007/s12350-017-0978-9

28. Pauwels EKJ, Sturm EJC, Bombardieri E, Cleton FJ, Stokkel MPM. Positron-emission tomography with [18F]fluorodeoxyglucose. Journal of Cancer Research and Clinical Oncology [Internet]. 2000 Sep 15;126(10):549–59. Available from: https://doi.org/10.1007/pl00008465

29. Scholtens AM, Verberne HJ, Budde RPJ, Lam MGEH. Additional Heparin Preadministration Improves Cardiac Glucose Metabolism Suppression over Low-Carbohydrate Diet Alone in ^{18}F-FDG PET Imaging. The Journal of Nuclear Medicine [Internet]. 2016 Apr 1;57(4):568–73. Available from: https://doi.org/10.2967/jnumed.115.166884

30. Sato K, Kawamatsu N, Yamamoto M, Machino-Ohtsuka T, Ishizu T, Ieda M. Utility of Updated Japanese Circulation Society Guidelines to Diagnose Isolated Cardiac Sarcoidosis. Journal of the American Heart Association [Internet]. 2022 Jun 29;11(13). Available from: https://doi.org/10.1161/jaha.122.025565

31. GE HealthCare. Discovery MI Gen 2 [Internet]. Available from: https://www.gehealthcare.com/products/molecular-imaging/pet-ct/discovery-mi-gen-2 Accessed January, 2024.

32. Schmidt M, Nuklearmedizinische Untersuchungen. In: Dietlein M, Kopka K, Schmidt M, editors. Nuklearmedizin Basiswissen und klinische Anwendung. 8th edition. Stuttgart (GER): Schattauer GmbH; 2017. p.108-128.

33. Madamanchi C, Weinberg RL, Murthy VL. Utility of serum ketone levels for assessment of myocardial glucose suppression for 18F-fluorodeoxyglucose PET in patients referred for evaluation of endocarditis. Journal of Nuclear Cardiology [Internet]. 2023 Jun 1;30(3):928–37. Available from: https://www.sciencedirect.com/science/article/abs/pii/S1071358123000417#preview-section-references

34. Balink H, Hut E, Van Der Pol T, Flokstra FJ, Roef MJ. Suppression of 18F-FDG myocardial uptake using a Fat-Allowed, Carbohydrate-Restricted diet. Journal of Nuclear Medicine Technology [Internet]. 2011 Jul 27;39(3):185–9. Available from: https://doi.org/10.2967/jnmt.110.076489

35. Özütemiz C, Koksel Y, Froelich JW, Rubin N, Bhargava M, Roukuz H, et al. Comparison of the effect of three different dietary modifications on myocardial suppression in 18F-FDG PET/CT evaluation of patients for suspected cardiac sarcoidosis. The Journal of Nuclear Medicine [Internet]. 2021 Mar 26;62(12):1759–67. Available from: https://doi.org/10.2967/jnumed.121.261981

36. Manabe O, Yoshinaga K, Ohira H, Masuda A, Sato T, Tsujino I, et al. The effects of 18-h fasting with low-carbohydrate diet preparation on suppressed physiological myocardial 18F-fluorodeoxyglucose (FDG) uptake and possible minimal effects of unfractionated heparin use in patients with suspected cardiac involvement sarcoidosis. Journal of Nuclear Cardiology [Internet]. 2015 Aug 5;23(2):244–52. Available from: https://doi.org/10.1007/s12350-015-0226-0

37. Sekiguchi M, Numao Y, Imai M, Furuie T, Mikami R. Clinical and Histopathological Profile of Sarcoidosis of the Heart and Acute Idiopathic Myocarditis Concepts through a study employing endomyocardial biopsy I. Sarcoidosis : Symposium on Secondary Myocardial Disease. The Nippon Journal of Angio-cardiology [Internet]. 1980 May 20;44(4):249–63. Available from: https://www.jstage.jst.go.jp/article/circj1960/44/4/44_4_249/_pdf/-char/en

38. Manabe O, Takahashi K, Kawakami H, Ohtsuka A, Aikawa T, Maki H, et al. Diagnostic values of delayed additional FDG PET/CT scan in the evaluation of cardiac sarcoidosis. Research Square (Research Square) [Internet]. 2023 May 24; Available from: https://doi.org/10.21203/rs.3.rs-2949688/v1

39. Chan WL, Ramsay SC, Szeto ER, Freund J, Pohlen JM, Tarlinton LC, et al. Dual-time-point 18F-FDG-PET/CT imaging in the assessment of suspected malignancy. Journal of Medical Imaging and Radiation Oncology [Internet]. 2011 Aug 1;55(4):379–90. Available from: https://doi.org/10.1111/j.1754-9485.2011.02287.x

40. Bermejo AP, Pardo FJP, Noriega-Álvarez E, Amo-Salas M, De Las Nieves Sicilia Pozo M, Vicente AMG, et al. Dual-Time-Point 18F-FDG PET/CT in Infective endocarditis: Impact of delayed imaging in the definitive diagnosis of endocarditis. Biomedicines [Internet]. 2024 Apr 13;12(4):861. Available from: https://doi.org/10.3390/biomedicines12040861

41. Tian R, Su M, Tian Y, Li F, Li L, Kuang A, et al. Dual-time point PET/CT with F-18 FDG for the differentiation of malignant and benign bone lesions. Skeletal Radiology

[Internet]. 2009 Feb 10;38(5):451–8. Available from: https://doi.org/10.1007/s00256-008-0643-0

42. Costantini DL, Vali R, Chan J, McQuattie S, Charron M. Dual–Time-Point FDG PET/CT for the evaluation of pediatric tumors. American Journal of Roentgenology [Internet]. 2013 Feb 1;200(2):408–13. Available from: https://doi.org/10.2214/ajr.12.8930

43. Zytoon AA, Murakami K, El-Kholy, El-Shorbagy E. Dual time point FDG-PET/CT imaging… Potential tool for diagnosis of breast cancer. Clinical Radiology [Internet]. 2008 Nov 1;63(11):1213–27. Available from: https://doi.org/10.1016/j.crad.2008.03.014

44. Uemura A, Morimoto S ichiro, Hiramitsu S, Kato Y, Ito T, Hishida H. Histologic diagnostic rate of cardiac sarcoidosis: Evaluation of endomyocardial biopsies. Am Heart J. August 1999;138(2):299–302. Available from: https://doi.org/10.1016/S0002-8703(99)70115-8

45. Simonen P, Lehtonen J, Kandolin R, Schildt J, Marjasuo S, Miettinen H, u. a. F-18-Fluorodeoxyglucose Positron Emission Tomography-Guided Sampling of Mediastinal Lymph Nodes in the Diagnosis of Cardiac Sarcoidosis. The American Journal of Cardiology. 2015 Nov;116(10):1581–5. Available from: https://www.sciencedirect.com/science/article/pii/S0002914915018524